Delamerian Reactivation of the Curnamona Province, Australia: age constraints and implications for the tectonothermal evolution from the retrograde shear zones

Rian Dutch*

*Continental Evolution Research Group, School of Earth and Environmental Sciences,

The University of Adelaide, Australia

Supervisor: Dr Martin Hand

Date: 10th day of November, 2003

Table of Contents

List of Figures

List of Tables

Abstract

Palaeoproterozoic to early Mesoproterozoic metamorphic rocks in the Curnamona Province are cross cut by a complex system of regional-scale retrograde shear zones that locally dominate the terrain. Combined metamorphic and geochronological data from localities across the southern Curnamona Province indicate that the peak metamorphic shear zone assemblages formed during the Cambrian Delamerian Orogeny, and not during the waning stages of ~1600Ma Olarian Orogeny as has been previously asserted. A combination of monazite chemical U-Th-Pb and garnet Sm-Nd geochronology indicates that shear zone fabrics formed between ~485 and 517Ma. Peak metamorphic conditions obtained from prograde garnet-staurolite-biotite-muscovite-chlorite-quartz assemblages are between 530 and 600°C at pressures of around 5 kbars. The absence of significant up-pressure prograde paths recorded by the mineral assemblages together with the modest (10-20%) degree of Delamerian shortening, suggests that attainment of burial to depths of around 15 km was largely a function of sedimentation associated with the development of the Adelaide Rift Complex between ~700-530 Ma. Metamorphic pressures within the shear zones in the central southern Curnamona Province suggest that Adelaidean sequence thicknesses there were in excess of 12 km prior to the Delamerian Orogeny. This estimate compares with previous estimates of <4 km for the thickness of Adelaidean cover in that part of the Curnamona Province and highlights the existence of unrecognised Adelaidean Rift Complex depocentres. The association between patterns of basement metamorphism and reactivation during the Delamerian Orogeny therefore reflects in part the distribution of pre-Delamerian sedimentation, and highlights the importance of pre-orogenic processes in controlling the style and pattern of terrain reactivation and reworking.

Key words: age constraints; Curnamona Province; Delamerian Orogeny; P-T conditions; shear zones; tectonothermal evolution.

1. Introduction

Due to the dynamic nature of the lithosphere and the comparative weakness of continental crust (e.g. Sandiford & Hand, 1998; Holdsworth et al., 2001), continental terrains often record numerous tectonothermal events, which effectively record the way in which the terrain underwent reactivation, or reworking (e.g. Hand & Buick, 2001; Holdsworth et al., 2001). Reactivation has been defined by Holdsworth et al. (1997) as *the accommodation of geologically separable displacement events (with intervals > 1 Ma) along pre-existing structures.* In a more general sense, reworking involves the repeated focusing of deformation, metamorphism and/or magmatism into the same volume of rock, so that every part of that volume has been affected or altered by the prevailing tectonothermal regime (Holdsworth et al., 2001; Krabbendam, 2001).

Unlike their wall rocks, which often preserve complex multi-event histories, shear zones tend to be the focus of intense deformation during reactivation (e.g. Grocott, 1977; Shaw and Black, 1991; Imber et al., 1997 D'Lemos et al., 1997; Needham and Morgan, 1997; Clendenin and Diehl, 1999) and therefore commonly preserve a detailed record of the conditions associated with reactivation (Murphy et al., 1999; Holdsworth et al., 2001). Because of this, the use of shear zones to determine the physical conditions associated with terrain reactivation is now firmly established (e.g. Ballevre et al., 2001; Scrimgeour and Raith, 2001). Used in this way, the structural, metamorphic and geochronological analysis of shear zone systems allows complex terrain histories to be unravelled and the tectonic framework associated with reactivation to be evaluated.

In using shear zones as a means to evaluate the tectonic history of a terrain, a key question that must be addressed is the absolute timing of shear zone development with respect to the age of earlier structures. Failure to constrain this parameter may lead to the formulation of apparent tectonothermal evolutions, where mineral assemblages developed within late-stage shear zones are linked to earlier assemblages (e.g. Warren, 1983; Dirks et al., 1991; Collins and Vernon, 1991). In many instances structural arguments, based on apparent geometric or kinematic similarities with earlier tectonic elements, have been used as a means to directly link the development of shear zone systems with the structural features they overprint (e.g. Dirks et al., 1991; Flint and Parker, 1993). However similarities in geometry and kinematic style between shear zones and earlier structures may be misleading, and reflect the role of the earlier structures in controlling the orientation and style of later and unrelated, shear zone systems (e.g. Marshak and Paulsen, 1996; Butler et al., 1995; Holdsworth et al., 1997; Imber et al., 1997; Holdsworth et al., 2001; Hand and Buick, 2001).

In terrains that lack obvious stratigraphic constraints on the timing of later shear zone systems, two somewhat coupled approaches can be employed to evaluate the tectonic relationship between shear zone systems and the structures they overprint. One obvious method is to directly date shear zone fabrics and their host structures with geochronometers that have closure systematics appropriate to the P-T conditions at which the structural fabrics form (e.g. Kreissig et al., 2001; Shaw et al., 2001; Streepee et al., 2001; Ballevre et al., 2001). The second method is to use metamorphic phase equilibria and mineral composition data to gauge the thermal history of shear zone fabrics, and whether they form part of the thermal evolution of the wall rock terrain (Ballevre et al., 2001; Scrimgeour and Raith, 2001).

A good example of a terrain that contains an extensive system of relatively late-stage shear zones that overprint a complex terrain history is the Curnamona Province in central southern Australia (Fig. 1). Within the Curnamona Province there are essentially two types of ductile shear zones. The first generation of shear zones are generally mica-rich, mid to low amphibolite grade. These have been reworked by greenschist grade mica-rich ductile shear fabrics. Most workers (e.g. Rutland and Etheridge, 1975; Glen et al., 1977; Berry et al., 1978; Laing et al., 1978; Corbett and Phillips, 1981; Clarke et al., 1986; Flint and Parker, 1993) have assumed that the amphibolite-grade shear zones formed during the cooling of the Palaeo-Mesoproterozoic (~1600-1590 Ma) Olarian Orogeny, which formed the wall rock terrain to the shear zone system. This assumption is in part based on structural arguments and limited thermochronological data (see sect. 3). An important consequence of this assumption is that amphibolite-grade mineral assemblages in the shear zones have been, in part, used to constrain the apparent anticlockwise PT evolution and isobaric cooling history for the Olarian Orogeny (Phillips and Wall, 1981; Clarke et al., 1987,1995). Most workers have also assumed that the later greenschist grade reworking is associated with the Cambrian Delamerian Orogeny (e.g. Berry et al., 1978; Flint and Parker, 1993), and have used this to make inferences about the grade of Delamerian-aged (~500Ma) metamorphism in the Proterozoic Willyama Supergroup (Fig. 1).

In this paper, metamorphic mineral assemblages that developed in shear zones across the Curnamona Province are described in detail. Seven locations have been chosen that cover an approximately 200km transect across the southern Curnamona Province, from the amphibolite grade Weekaroo region to the granulite grade Broken Hill area (Fig. 2). At each location the metamorphic evolution is documented, and age constraints on the timing of shear zone metamorphism provided. The results of this study suggest that:

(1) The amphibolite-grade shear zone that characterise much of the Curnamona Province formed, or were reactivated at their peak recorded PT conditions, during the Cambrian Delamerian Orogeny, and should not be included in Proterozoic terrain evolution models.

(2) The Cambrian-aged shear zone mineral assemblages are essentially identical to those used to constrain the early Mesoproterozoic apparent anticlockwise isobaric cooling PT path of the Olarian Orogeny (Phillips and Wall, 1981; Clarke et al., 1987). This similarity casts significant doubt on the inferred Olarian P-T evolution, and suggests it may be an artefact resulting from the overprinting of Proterozoic mineral assemblages by Cambrian assemblages during Delamerian-aged terrain reactivation.

(3) The Cambrian-aged metamorphism in part reflects the thickness distribution of the Neoproterozoic Adelaidean cover sequences, which overlay the Proterozoic basement rocks that host the Cambrian-aged shear zone assemblages.

2. Geological Setting

The Curnamona Province (Fig. 1) is recognised internationally for containing several important mineral deposits, including the world class Pb-Zn-Ag deposit at Broken Hill, which is hosted within granulite-grade rift-related sequences belonging to the Palaeoproterozoic Willyama Supergroup (Laing et al., 1978; Morland and Webster, 1998). The Curnamona Province has been sub-divided into the Broken Hill and the Olary Domains (Stevens, 1986; Fig. 1), however stratigraphic and tectonic correlations are well established (e.g. Page et al., 2000, 2003), and the division is somewhat artificial. The geology of the Olary Domain has been summarised by

Clarke et al. (1986, 1987), Cook and Ashley (1992), Flint and Parker (1993), Robertson et al. (1998), Conor (2000) and Raetz et al. (2002). The Geological evolution of the Broken Hill Domain has also been the focus of numerous studies (e.g. Vernon, 1969; Laing et al., 1978; Marjoribanks et al., 1980; Willis et al., 1983; Stevens, 1986; Raetz et al., 2002).

The general tectonic character of the Curnamona Province reflects the ~1610-1590Ma Olarian Orogeny, which was a compressional tectonic interval characterised by high heat flow, producing regional low-pressure high-temperature amphibolite to granulite grade mineral assemblages (Laing et al., 1978; Marjoribanks et al., 1980; Clarke et al., 1987, 1995). The complex structural and metamorphic record resulting from the Olarian Orogeny has been overprinted by a terrain-scale system of greenschist to amphibolite grade ductile retrograde shear zones that locally dominate the structural and metamorphic character of the province (Fig. 2).

2.1. Curnamona Province shear zones

The Curnamona Province shear zones, commonly called retrograde schist zones (e.g. Stevens, 1986; Clarke et al., 1986), are typically steeply-dipping, curviplanar zones, characterised by an intense schistosity that is at a lower grade than the surrounding host wall rocks. In the Olary and Broken Hill Domains, the shear zones form a conjugate system, generally trending either E-W to SE-NW, or NNE-SSW (Fig. 2), and typically contain steeply-plunging mineral lineations, with movement sense generally SW or SE up (e.g. Vernon and Ransom, 1971; Bottrill, 1998; Wilson and Powell, 2001; Williams and Vernon, 2001).

The shear zones vary in width from a few metres to over 2 kilometres wide, with zones being widest in the Broken Hill Domain, where they form large-scale schist belts. Individual shear zones can be traced for kilometres in outcrop, but can be seen for tens of kilometres on Landsat imagery and in airborne geophysical data. Despite being a volumetrically significant part of the terrain, and linking with a crustal scale shear zone system (Leven et al., 1998), there are comparatively few direct age constraints on the timing of the shear zones or descriptions of their metamorphic character and evolution.

There are important regional variations in metamorphic grade of the shear zone system. In the southern Broken Hill and southeastern Olary domains, the shear zones contain amphibolite-grade assemblages characterised by coarse-grained 2-mica-staurolite-bearing assemblages that may contain garnet or kyanite (e.g. Vernon and Ransom, 1971). Locally there are spectacular garnet-chlorite-bearing assemblages, with abundant euhedral garnet porphyroblasts up to 20 cm in diameter. Westwards and northwards, the grade of the shear zones decreases to greenschist-grade assemblages (Laing, 1996), concomitant with a general decrease in the width of the shear zones.

3. Existing constraints on the timing of shear zone development in the Curnamona Province

The timing of retrograde shear zone (RSZ) development in the Curnamona Province has been a matter of some discussion for the past 30 years (e.g. Vernon and Ransom, 1971; Willis, 1976; Laing, 1977, 1996; Glen et al., 1977; Corbett and Phillips, 1981). Various lines of evidence have been used to attribute the majority of the RSZ to the retrograde stage (OD_3) of the 1600-1590 Ma Olarian Orogeny (e.g. Marjoribanks et al., 1980; Laing et al., 1978). Various authors (e.g. Willis, 1976; Laing, 1977, 1996; Glen et al., 1977; Corbett and Phillips, 1981) have suggested that the RSZ's are an extension of the OD_3 event, due to a general spatial correspondence of the peak metamorphic Olarian grades with the grades of the RSZ's (Fig. 3). These authors also suggested that the general parallelism between the local orientations of the OD_3 retrograde schistosity and shear fabrics in the RSZ's points to similar timing. Several structural studies (e.g. Bottrill, 1998) have also shown that some of the RSZ are apparently truncated at the Adelaidean unconformity, and therefore must predate the deposition of these Neoproterozoic sediments

Although the structural and metamorphic evidence indicating an Olarian (~1600-1590Ma) age for the RSZ appears convincing based on the above evidence, there is little direct geochronological data on formation of the RSZ mineral assemblages. To add to the ambiguity over the age of the shear zones, there is also evidence pointing to important Delamerian-aged (Cambrian), and possibly late Mesoproterozoic events in the Curnamona Province. Firstly, structural evidence suggests that many of the shear zones may be largely Delamerian in age based on the general absence of folding of shear zones by events including the Delamerian Orogeny (Stevens, 1986). Similarly Laing (1969) and Lishmund (1982) showed that the many of the shear zones disrupt the Adelaidean cover sequences. Secondly, Sm-Nd data from a garnet-mica schist from the Walter-Outalpa Shear Zone gives an apparent Delamerian age of 509 ± 20 Ma (Bottrill, 1998).

Isotope studies undertaken on rocks from the Curnamona Province present apparent evidence for a number of thermal events in the province. Ar-Ar suggests that three thermal pulses have affected the region. The first event, was the Olarian Orogeny

(~1600-1500 Ma), which is recorded by apparent cooling ages in the range 1550-1500 Ma (Harrison and McDougall, 1981). The second event is based on a cluster of Grenvillian-aged (1200-1100 Ma) Ar-Ar mineral ages (Lu et al., 1996; Hartley et al., 1998). However, as yet, there is no identified structural or metamorphic expression of this apparent thermal event, but an obvious possibility is that some of the Curnamona Province retrograde shear zones either formed, or were reactivated at this time. The third recognised thermal event is the ca. 500 Ma Delamerian Orogeny (Harrison and McDougall, 1981; Lu et al., 1996; Hartley et al., 1998). A considerable amount of isotopic data points to increased temperatures during the Delamerian Orogeny. Bierlein et al. (1996) presented Ar-Ar data from mineralised veins and shear zones from the Olary Domain that gave a Delamerian age for epithermal mineralisation and tectonothermal activity. K-Ar analyses of hornblende and biotite from the Broken Hill region by Harrison and McDougall (1981) gave an age of 535 ± 5 Ma, which is consistent with K-Ar ages of around 500 Ma obtained by Richards and Pidgeon (1963). Harrison and McDougall (1981) also present Rb/Sr data from 14 analysed biotite samples which give an age of 520 ± 35 Ma, consistent with Rb/Sr data on retrograde muscovite from the mine sequence at Broken Hill, which gives an age of ~484 Ma (Pidgeon, 1967), and Rb/Sr ages of between 466 Ma and 488 Ma obtained on biotites from psammopelitic gneisses in the Broken Hill Domain (Page and Laing, 1992). Although this data present a convincing case for the importance of the Delamerian Orogeny as a thermal event in the Curnamona Province, very little of the existing thermochronological data is directly applicable to the amphibolite grade shear zone assemblages. This is because the bulk of the data relates to isotopic systems with closure temperatures ~200°C lower than the likely peak metamorphic temperatures (~500-600°C) recorded in the shear zones.

4. Brief geological descriptions of selected shear zone locations

Seven areas from across the southern Curnamona Province were selected covering a total east-west distance of around 200 km. The locations were chosen to document type examples of retrograde shear zones across the province.

4.1. Southwestern Olary Domain

The Walter-Outalpa Shear Zone (Fig. 2) is an approximately 10 km long, 100 to 400m wide zone of highly schistose metapelite and metapsammite outcrops. The shear fabric trends ESE and dips steeply (~80º) south, and contains a down-dip mineral stretching lineation (L_x), defined by micas. Shear-sense indicators (SC bands) indicate top to the north movement. On its eastern end, the shear zone appears to be truncated by the Adelaidean unconformity, however along its western extension, the Adelaidean sequences are locally overturned, and contain a biotite schistosity.

4.2. Southeastern Olary Domain

The Kings Dam Shear Zone (Fig. 2) is an approximately 30 km long, 500m wide, E-W trending schist belt that crosscuts upper amphibolite grade Willyama Supergroup metasediments. Outcrop of this structure is poor to non-existent, but it is sharply defined in aeromagnetic images. Dips are poorly constrained, however they are likely to be steep, in keeping with the bulk of the Curnamona Province shear zones. NE trending Olarian D_3 (~1590 Ma) folds have been dragged into an E-W orientation aligned with the shear zone, indicating an apparent 4 kilometres of dextral transcurrent displacement. Due to the lack of outcrop, the amount of vertical movement has not been determined, as the orientation of the stretching lineation is unknown.

The Mutooroo Shear Zone (Fig. 2) is a diffuse, roughly E-W trending structure which is approximately 15 kilometres long. Like the Kings Dam Shear Zone, outcrop is poor, but the structure can be seen in aeromagnetic data. The Mutooroo Shear Zone has a steeply plunging mineral elongation lineation however the sense of movement is unknown.

4.3. Southwestern Broken Hill Domain

The Thackaringa-Pinnacles Shear Zone (Fig. 2) has a strike length of around 15km and is a complex system of anastomosing micaceous shear zones trending roughly E-W. The shear zone system is approximately 4 kilometres wide, and cuts across granulite and upper amphibolite-grade rocks of the Broken Hill Domain. This structure is steeply south-dipping, with a steep mineral lineation. However due to poor outcrop, the sense of movement has not been determined.

The Pinnacles area, south west of Broken Hill, is characterised by a highly sheared package of granulite grade Willyama Supergroup sequences (Figs. 2 and 4). Shear zones range from 10m to >100m in width, and generally display a south side up sense of movement. A number of the shear zones have been sampled for this study, using both surface outcrop and drill core from the Pinnacles Mine lease. This area contains steeply-dipping E-W trending shear zones (e.g. the Theta shear and Consols shear, Fig. 4) and the NW-SE trending Pine Creek and Pinnacles zones (Fig. 4).

4.4. Broken Hill district

The Stephens Creek Shear Zone (Fig. 2) has been the focus of a number of studies (e.g. Vernon and Ransom, 1971; Wilson and Powell, 2001), and is considered to be a type example of retrograde shear zone development in the Curnamona Province. It is a steeply south-dipping E-W trending zone approximately 250 metres wide, that can be traced for ~15km. The shear zone cuts through predominantly upper amphibolite facies metapelites and felsic gneisses of the Sundown and Broken Hill Groups (Stevens and Bradley, 1993). The shear fabric contains a steeply-plunging mineral elongation lineation defined by micas, and appears to have formed during south-side up displacement; however the magnitude of movement has not been constrained.

5. Petrography

In this section, the mineral assemblages developed at the selected locations across the southern Curnamona Province are described as a basis for thermobarometric and mineral equilibria analysis. The selected regions range in metamorphic grade from upper greenschist to amphibolite grade and were chosen to cover much of the regional E-W variation in metamorphic grade and style of retrograde shear zone development.

The chosen assemblages are, with one exception, metapelitic in composition. The assemblages for each location are detailed in Appendix 1. Generally the assemblages contain quartz + muscovite + biotite + ilmenite ± chlorite with minor apatite, zircon and monazite. In addition to these matrix-forming minerals, the metapelitic shear zone assemblages used in this study all contain garnet, and also typically staurolite and plagioclase.

5.1. Textural characteristics of the main mineral phases

Samples used in this study have been separated into three groups depending on the textural characteristics.

5.1.1. Group 1

This group includes the Walter-Outalpa, Pinnacles and Stephens Creek shear zones. Mineral assemblages consist of inter-layered mica-rich and quartz-rich layers, which show variable degrees of dynamic recrystallisation. Fine-grained muscovite, chlorite and biotite with minor ilmenite (Fig. 5a, b and c) define a well-developed foliation. Muscovite and biotite crystals up to 1mm in length also occur in the quartz-rich layers along with minor plagioclase. Garnet occurs as anhedral to subhedral porphyroblasts, generally up to 2mm in diameter but can reach almost a centimetre in some samples. Garnet contains inclusions of quartz, ilmenite and sometimes clinozoisite. The external fabric (S_e) wraps around the garnet porphyroblasts, creating strain caps and pressure shadows (Fig. 5c). These pressure shadows often contain coarse-grained plagioclase, quartz, muscovite and biotite crystals. Curved and spiral inclusion trails within garnet suggest syn-tectonic growth (Fig. 5b). Staurolite porphyroblasts range from sub-millimetre size in samples from the Pinnacles Mine region, to centimetre size from the Stephens Creek Shear Zone (Fig. 5a). Locally staurolite overgrows garnet, suggesting that staurolite growth occurred after garnet, and continued later into the deformational history. The shear fabric is cross-cut by porphyroblasts of muscovite and chlorite up to 1 mm in size.

5.1.2. Group 2

This group consists of the Kings Dam Shear Zone. Group 2 samples are similar in style to samples in Group 1 but tend to contain more quartz, and significantly more garnet and staurolite (Fig. 5d and e). Similar to Group 1 they have inter-layered micaceous-rich cleavage layers with quartz rich microlithons. Fine-grained biotite, muscovite and recrystallised quartz grains define the shear foliation. Subhedral to euhedral garnets range in size from 0.5 to 2cm in diameter. Inclusion trails in garnet consist of quartz and ilmenite, and range from slightly curved to closed spirals. Staurolite crystals up to 5mm long occur both as overgrowths on garnet, and isolated within the matrix. Staurolite crystals are contained both within the foliation and cross cut it (Fig. 5e). This suggests that staurolite continued to grow later than garnet, and also post-kinematically. Some late chlorite and muscovite porphyroblasts up to 1mm in length also cross-cut the foliation (Fig. 5d).

5.1.3. Group 3

This group consists of the Thackaringa-Pinnacles and Mutooroo shear zones. Group 3 shear zone assemblages contain a coarse grained matrix of chlorite, biotite and plagioclase crystals up to 1cm long with minor ilmenite (Fig. 5f). The foliation is defined by chlorite and ilmenite and both quartz-bearing and quartz-absent varieties occur. Garnet occurs as euhedral porphyroblasts ranging from 0.5cm to greater than 20cm in diameter. Garnet contains inclusions of plagioclase, ilmenite, staurolite and hornblende (Fig. 5f). Curved inclusion trails within garnet suggest growth was syn-tectonic with the shear zone development. Pressure shadows adjacent to garnet porphyrobalsts contain large biotite crystals up to 1cm in length. Plagioclase appears to pre date-biotite and chlorite, as it occurs as inclusions in both.

6. Mineral Chemistry

Mineral compositions for each of the selected RSZ's were obtained using a Cameca SX51 Electron Microprobe, at Adelaide Microscopy, located at the University of Adelaide. Quantitative analyses were run at an accelerating voltage of 15 kv and a beam current of 20 nA. Representative mineral compositions are shown in Table 1.

Muscovite from all selected areas has an XFe of ~0.05, an XNa from 0.08 to 0.21 and an Al^{VI} of 1.68 to 1.82 (based on 11 oxygens). Biotites have XFe^{2+} (annite) values that range between 0.39 to 0.74, XNa of ~0.04, XTi from 0.06 to 0.2 and an Al^{VI} of 0.2 to 1.16 (based on 11 oxygens). Syn-kinematic chlorite defining shear fabrics in garnet-chlorite belts (e.g. Thackaringa-Pinnacles, Mutooroo and Walter-Outalpa RSZ) has an XFe of 0.34 to 0.5, an XMg of 0.14 to 0.43 and an Al^{VI} of 1.17 to 1.37 (based on 14 oxygens). Plagioclase compositions range from albite 0.64 to 0.81 and anorthite 0.18 to 0.35 (based on 8 oxygens), with the most Ca-rich compositions occurring in the Walter-Outalpa RSZ. Staurolite cores and rims typically have an XFe of ~0.84 and an Al^{VI} of 8.91 (based on 46 oxygens). Garnet cores have an XFe from 0.29 to 0.91 and an XMn of 0.001 to 0.5, rims have an XFe typically between 0.41 to 0.9 and an XMn of 0.004 to 0.45 (based on 8 oxygens). The most Fe-rich compositions come from the Kings Dam and Thackaringa-Pinnacles RSZ, where as Mn-rich garnets characterise the other selected RSZ's.

In order to further explore the compositional character of garnets from the Curnamona Province shear zones, individual garnets were compositionally mapped for the elements Fe, Mg, Mn and Ca, prior to quantitative analysis. Qualitative cation mapping using an SX51 Electron Microprobe ran at an accelerating voltage of 15 kv and a beam current of 80 nA. All analysed garnets had core to rim cation concentration distributions characteristic of prograde growth zoning (Fig. 6; e.g. Spear, 1993). None of the mapped garnets had zoning patterns that were suggestive of significant intra-crystalline diffusion (e.g. Florence and Spear, 1991). Compositional mapping also shows that there was no evidence of retrograde net transfer reactions that would significantly affect thermobarometric results (e.g. Kohn and Spear, 2000).

7. P-T conditions of shear zone formation

Pressures and temperatures for the formation of the selected shear zone assemblages were calculated via the average-P and average-T approach (Powell and Holland, 1994) using the computer program THERMOCALC v3.1 (Powell and Holland, 1988) and the 1999 update of the Holland and Powell (1998) internally consistent dataset. Activity-composition relationships for minerals used in calculations were calculated using the software AX2000 (Powell and Holland, 1998). Appendix 2 contains an example AX2000 output file, an example THERMOCALC output file can be seen in Appendix 3.

The P-T conditions for the formation of each of the selected RSZ's are summarised in Table 2. For all shear zones, the calculated P-T conditions are generally between 530°C to 600°C at around 5 to 5.5 kbars. However individual uncertainties on mineral calculations may be up to ± 100°C at 1σ (Table 2). In order to reduce the uncertainties, a number of samples have been analysed from each location, and their P-T conditions of formation averaged (at 2σ). In this way the mean P and T can be used, and the uncertainties pooled to reduce the error (Table 2).

Since the shear zone mineral assemblages all contain hydrous minerals, and the overall assemblages are more hydrous than the surrounding wall rocks, it is likely that a free fluid phase was present during shear zone metamorphism. In this case, the composition of the fluid may exert a strong influence on the apparent P-T stability of the observed mineral assemblages (e.g. Spear, 1993; White et al., 2003). In order to explore this dependency, P-T calculations were undertaken using a range of assumed fluid compositions modelled as H_2O-CO_2 mixtures that define XH_2O in the fluid. The Walter-Outalpa Shear Zone assemblages were chosen as a case study. Figure 7a shows that as XH_2O is decreased, calculated pressures increase from 5 kbars at XH_2O = 1 to > 6 kbars at XH_2O = 0.2. Calculated temperatures follow the opposite trend, decreasing from ~530°C at XH_2O = 1 to ~400°C at XH_2O = 0.1 (Fig. 7b). The comparatively precise estimate for pressure in the Walter-Outalpa RSZ (5 ± 0.8 kbar 2σ) using XH_2O = 1 is similar to that implied by the thickness of the overlying Adelaidean cover sequence (~10-12 km; see below). This suggests that fluids in the Walter-Outalpa RSZ had compositions close to XH_2O = 1, and therefore temperature calculations should incorporate a high XH_2O fluid. In the case of the Walter-Outalpa Shear Zone, calculations using XH_2O = 1 gives peak temperatures of around 530°C.

.

8. Age constraints on the formation of RSZ assemblages

In order to provide direct age constraints on the formation of the Curnamona Province RSZ's a combination of garnet Sm-Nd and monazite chemical U-Th-Pb geochronology were used.

8.1. Sm-Nd Geochronology

Garnet Sm-Nd geochronology was undertaken on samples from the Kings Dam, Mutooroo and Thackaringa-Pinnacles RSZ's (Fig. 2). Prior to analysis, garnets were compositionally mapped to determine whether they had undergone significant intra-crystalline diffusion (e.g. section 5; Fig. 6). The presence of diffusional zoning would indicate that the garnets had experienced temperatures at or above the closure temperature of the Sm-Nd isotopic system for a significant time (e.g. Burton et al., 1995; Becker, 1997; Mawby et al., 1999). Estimates of the closure temperature (T_c) in garnet range between ~650 °C and 900 °C for a cooling rate of 10 °C Ma^{-1} (Mawby et al., 1999, and references therein). Samples were also selected on the criteria that they contained minimal oxide, and no epidote inclusions, which can lead to significant analytical contamination.

Once rock samples for analysis had been selected they were crushed, milled and sieved and mineral fractions separated via magnetic and heavy liquid separation techniques. Dr Jo Mawby carried out isotopic analysis at the Geology and Geophysics isotope facility at the University of Adelaide. Surface contamination on the handpicked mineral separates was removed by an ultrasonic cleaner in 1M HCl solution. Between 125 and 300mg and 100-150mg of sample was used for mineral separates and whole rock samples respectively. The mineral separates were milled under ethanol in an agate mortar to a grainsize < ~2 microns. To minimise contamination of mineral fractions by REE-rich inclusions, the milled fractions were leached in hot HF for one hour. The leachate was pipetted from the residual solid material and the solid material washed three times in cold 6M HCl separately to remove any trace of the leachate fraction. For the whole rock component, around 150mg of milled whole rock was dissolved in HNO_3 - HF acid mixtures for periods between 1 and 10 days. All samples were spiked with a mixed ^{147}Sm-^{150}Nd spike prior to dissolution. Nd and Sm isotopic compositions were measured on a Finnigan MAT 262 TIMS in static mode. The isotopic ratios were corrected for fractionation to ^{146}Nd/^{144}Nd = 0.7120903 and to a ^{152}Sm/^{149}Sm ratio of 1.9347. Spiked samples of BCR-1 yielded a ^{143}Nd/^{144}Nd ratio of 0.512598 ± 17 after spike unmixing. Reported errors on the measured ^{143}Nd/^{144}Nd are 2 standard error analytical uncertainties. The ^{143}Nd/^{144}Nd reproducibility of the internal standard over the course of the study (n = 10) was 0.511602 ± 0.00001. For age calculations Sm/Nd errors were estimated to be ± 0.3%. Isochron calculations were done using Isoplot v. 2.49 (Ludwig, 2001) with ages (reported at 95% confidence) based on a decay constant for ^{147}Sm of 6.54 x $10^{-12}y^{-1}$. The total procedural Sm and Nd blanks were < 0.5 mg.

All geochronological results are summarised in Table 3. From the Kings Dam RSZ 3 individual syn-tectonic euhedral garnets up to 1.5 cm in diameter were analysed. The garnets and their leachates together with the whole rock give an age of 505 ± 13Ma. The Mutooroo RSZ is a quartz poor assemblage dominated by chlorite that envelops euhedral garnets up to 3 cm in diameter (Fig. 5b). Analysis of a garnet and the whole rock gives an age of 517 ± 14Ma. A third sample from the Thackaringa-Pinnacles RSZ was analysed. A single euhedral garnet, 12 cm in diameter from a chlorite schist, containing inclusions of orthoamphibole and staurolite was slabbed and the core and rim analysed, giving an age of 500 ± 10Ma.

8.2. Monazite U-Th-Pb Geochronology

Monazite U-Th-Pb chemical dating (e.g. Montel et al., 1996; Williams and Jercinovich, 2002) was undertaken on samples of metapelitic schists from the Thackaringa-Pinnacles and Stevens Creek RSZ's (Fig. 8a). The geochronological technique is based on the chemical dating of monazite, using an electron microprobe to measure the amounts of U, Th and Pb. Monazite is typically very rich in the radioactive elements U and Th, and therefore radiogenic Pb accumulates at a rate such that measurable quantities (>300 ppm) of Pb are reached in about 100 Ma (Montel et al., 2000). Previous studies (e.g. Parrish, 1990) have demonstrated that monazite contains negligible common Pb compared with the radiogenically produced component, therefore it can be assumed that all measured Pb in monazite is the result of the radiogenic breakdown of Th and U. The most recent estimate of the closure temperature for Pb diffusion in monazite is ~900 °C at a cooling rate of 10 °C/Ma in a 10 μm grain (Pyle et al., 2003). Thus monazite is a useful dating tool for the amphibolite grade rocks of the Curnamona Province RSZ's, since it is almost certain to record growth ages.

Analyses of monazite were conducted using a Cameca SX51 Electron Microprobe, at Adelaide Microscopy in the University of Adelaide. The analysis was run at an accelerating voltage of 20 kV and a 50 nA beam current. Th, U and Pb were analysed concurrently with PET crystals using Mα lines for Th and Mβ lines for Pb and U. The standards used were huttonite (Th), UO_2 and a synthetic Pb glass. The full range of elements which are typically partitioned into monazite were analysed (Table 4), and analyses below 97% total concentration were rejected for age determination. Offline corrections were made to account for the overlap of the second order Ce Lα escape peak with the required Pb Mβ peak (Pyle et al., 2003). The ages for each spot were then determined using the U-Th-Pb concentrations, and the statistical methods outlined in Montel et al. (1996). Probe performance was monitored by comparison with a standard 514 Ma monazite with known U-Th-Pb concentrations. Reproducibility of the standard (n = 38) was 504 ± 47 Ma.

All ages are summarised in Table 3. Analysed monazites were typically subhedral grains up to 50μm long (Fig. 8a). Two samples (Sr2 and WTP1) from the Thackaringa-Pinnacles RSZ (Fig. 2) were analysed. In both samples the monazite grains were located within the matrix shear foliation and also as inclusions in garnet. Sample Sr2 from the eastern end of the Thackaringa-Pinnacles RSZ produced a pooled metamorphic age of 499 ± 36Ma (2σ) with a MSWD of 0.19. Sample WTP1 from the western end of the Thackaringa-Pinnacles RSZ produced a pooled age of 498 ± 78Ma (2σ) with a MSWD of 0.083 (Fig. 8b and c). If the two samples are combined, a pooled age of 499 ± 32Ma is obtained. In the Stephens Creek RSZ (SCS5; Fig.2), monazites located within the shear fabric give a pooled age of 485 ± 53Ma (2σ) with a MSWD of 0.15 (Fig. 8d).

9. Discussion

9.1. Timing of shear zone metamorphism

The age constraints on amphibolite-grade shear zone assemblages from across the Curnamona Province derived from monazite U-Th-Pb chemical dating and garnet Sm-Nd dating, show that the peak shear zone assemblages formed during the Cambrian Delamerian Orogeny. The ages obtained in this study are consistent with the apparent Delamerian ages derived from garnet Sm-Nd analysis and reconnaissance monazite U-Th-Pb from the Walter-Outalpa and associated shear zones (Bottrill 1998; L. Rutherford, pers comm Sept 2003) in the western Curnamona Province. Therefore Delamerian ages have now been obtained from shear zones across the entire southern Curnamona Province. The Delamerian ages suggest that, strictly speaking, the shear zones should not be regarded as retrograde, since they must have undergone a prograde (mostly T increasing) metamorphic evolution, consistent with the prograde zoning recorded in shear zone garnet (Fig. 6).

Existing isotopic data (see sect. 3) from rocks across the Curnamona Province suggest that three tectonothermal events have affected the Willyama Supergroup metasediments. These events are the ~1600 Ma Olarian Orogeny, an event during the Grenvillian (~1200-1100 Ma), and the ~500 Ma Delamerian Orogeny. The preservation of apparent Olarian-aged Ar-Ar ages from the Broken Hill Domain granulites (Harrison and McDougall, 1981) probably reflects the grade of subsequent tectonothermal events. RSZ's in the Broken Hill Domain only reach middle amphibolite facies conditions (~550°C). In the granulitic blocks between the shear zones, micas would have largely escaped later recrystallisation, and appear to preserve near Olarian Ar-Ar ages despite being heated to above their nominal Ar-Ar closure temperatures of around 300-400°C (e.g. Harrison and McDougall, 1981; Foster and John, 1999). The presence of an apparent Grenvillian aged thermal event is based on a cluster of Ar-Ar ages in the range 1200-1100 Ma (Hartley et al., 1998; Lu et al., 1996), and is synchronous with the large scale Musgravian event in central southern Australia (e.g. Camacho and Fanning, 1995). The identification of Ar-Ar ages in this range introduces the possibility that the Curnamona Province RSZ's formed, or were reactivated at this time. Structural evidence, for example the truncation of the Walter-Outalpa RSZ at the Adelaidean unconformity (Bottrill, 1998), suggests that at least some of the RSZ's must have formed prior to the ~700 Ma deposition of the Adelaidean sequences (Preiss, 2000). A Musgravian age for the retrograde shear zones would allow the mineral assemblages within the zones to form during prograde metamorphic paths, consistent with garnet zoning patterns (Fig. 6). However, no geochronological data was found in this study to support pre-Delamerian ages, suggesting that these pre-Adelaidean shear zones formed at lower grades than the Delamerian reworking.

9.2. Metamorphic phase equilibria

Petrological observations of the sequence of mineral growth in the RSZ assemblages can provide important constraints on the P and T of formation when interpreted in relation to the positions of mineral stability fields in PT pseudosections of appropriate bulk compositions (e.g. Alias et al., 2002; Stuwe and Ehlers, 1997; Mahar et al., 1997). The petrological evolution of the RSZ's (discussed in sect. 5) indicates that either staurolite grew before garnet (in the case of Thackaringa-Pinnacles) or, more commonly, garnet growth occurred before staurolite. In the case of the Kings Dam RSZ, staurolite growth appears to be both syn- and post-kinematic with respect to the shear fabric, and in all cases there is late chlorite.

The Kings Dam and Thackaringa Pinnacles RSZ's are sub-aluminous Fe rich pelitic assemblages with a small Mn component (~0.01% MnO whole rock composition). Therefore the metamorphic phase equilibria can be modelled using an appropriate PT pseudosection in the KFMASH (K_2O-FeO-MgO-Al_2O_3-SiO_2-H_2O) system (Fig. 9). Typically, the RSZ's in the Curnamona Province have a higher MnO component (up to 0.4% MnO whole rock composition) and therefore cannot be effectively modelled using the KFMASH system. These Mn-rich RSZ's have been analysed using a pseudosection based in the system MnKFMASH (MnO_2-K_2O-FeO-MgO-Al_2O_3-SiO_2-H_2O) system (Fig. 10). The effect of Mn on the topology of mineral stability fields in PT space has been investigated by a number of authors (e.g. Spear and Cheney, 1989; Dymoke and Sandiford, 1992; Symmes and Ferry, 1992; Mahar et al., 1997; Pattison et al., 1999). In particular, in the system MnKFMASH, garnet is stabilised at lower pressures and temperatures over a wide range of bulk compositions (Symmes and Ferry, 1992; Mahar et al., 1997). Many of the RSZ assemblages sampled in this study contain the association garnet-chlorite-biotite (+ muscovite and quartz). In the system MnKFMASH, this assemblage is stable at the PT conditions derived from thermobarometry (Table 2; Fig. 10; Mahar et al., 1997), suggesting that the pseudosection in Figure 10 is appropriate to describe the petrological evolution of the Mn-bearing shear zone assemblages.

In the Kings Dam RSZ, the observed assemblage (staurolite-garnet-chlorite-muscovite-quartz + late staurolite and chlorite) plots within the staurolite-garnet-chlorite-muscovite field of PT space (Fig. 9). Importantly this divariant assemblage is located at around the PT conditions derived from thermobarometry, suggesting the PT pseudosection in Figure 9 is appropriate for modelling the PT evolution of the Kings Dam RSZ. Aside from the presence of prograde zoned garnet, there is no textural remnant of the prograde mineral assemblages. The continued growth of staurolite after garnet suggests that the PT path evolved in a decompressive manner (Fig. 9) in order to account for the increase in staurolite modes, leading to the establishment of a staurolite-chlorite-muscovite assemblage toward the end of the deformation.

Samples from the Thackaringa-Pinnacles RSZ preserve an initial assemblage of staurolite and chlorite (found as inclusions in garnet) which was overgrown by garnet with staurolite and chlorite. This suggests that the rocks may have started in the staurolite-chlorite-muscovite field and tracked up T and slightly up P into the staurolite-garnet-chlorite-muscovite field (Fig. 9). Therefore a composite picture of both the prograde and retrograde Delamerian evolution of Curnamona shear zones can be pieced together by combining the textural records of the Kings Dam and Thackaringa-Pinnacles Shear Zones. The remaining RSZ samples all show an up T path from the garnet-biotite-chlorite field into the garnet-staurolite-chlorite-biotite and then the garnet-staurolite-biotite fields (Fig. 10).

There are two important implications of these inferred PT paths. Firstly, the peak metamorphic shear zone assemblages all plot within the kyanite stability field in PT space. Secondly, there is no evidence of lower P or T assemblages which precede the observed peak assemblages (apart from those seen in the samples from Thackaringa-Pinnacles, which still formed at conditions above 500 °C). This suggests that the shear zone volumes may have already been at depth prior to their formation/reactivation (discussed in section 9.3.).

The first observation (above) has significant implications for the inferred evolution of the 1600-1590Ma Olarian Orogeny. Previous workers have used the existence of apparent late-stage kyanite in the terrain to indicate an anticlockwise PT path with isobaric cooling for the thermobarometric evolution of the Olarian Orogeny (e.g. Phillips and Wall, 1981; Clarke et al., 1987). In places, the kyanite-bearing assemblages occur in the RSZ that form part of the shear zone system in the Broken Hill region, which gives Delamerian ages for peak shear zone metamorphism. This study has shown that PT conditions in the Willyama Supergroup rocks during the Delamerian Orogeny would have allowed the growth of kyanite in rocks of appropriate composition. This suggests that the presence of kyanite in the terrain may be a result of Delamerian metamorphism. This puts the inferred trajectory of the Olarian PT path (e.g. Phillips and Wall, 1981; Clarke et al., 1987) in some doubt, as the key mineral phase used to determine the retrograde path might have actually formed around 1000Ma after the Olarian Orogeny. The suggestion that the Olarian PT evolution is not anticlockwise is also supported by recent interpretations of the Olarian-aged mineral assemblages which suggest that the PT evolution of the Olarian Orogeny may be clockwise in character (Hand et al., 2003; Swapp & Frost, 2003).

9.3. The role of Adelaidean cover sequences in Delamerian-aged shear zone metamorphism

In general, the attainment of peak pressure conditions in compressional systems such as the Delamerian Orogeny reflects the affects of crustal thickening (e.g. Wilson et al., 1992; many others). Within this context, constraints on the amount of Delamerian shortening have important implications for the mechanisms that lead to the burial depths recorded in the shear zone assemblages. Delamerian-aged folds expressed in the Adelaidean cover overlying the Willyama Supergroup are in general open to locally tight, but do not reflect large-scale shortening (e.g. Clarke et al., 1986;

Berry et al., 1978). In the Weekeroo Inlier region in the southwestern Curnamona Province estimates of Delamerian shortening are in the order of 10-20% (Paul, 1998; Paul et al., 1999). This amount of shortening is insufficient to cause significant burial of the basement that hosts the shear zones. The implication of this is that significant burial of the basement must have occurred prior to the Delamerian Orogeny. The most obvious pre-Delamerian burial mechanism is Adelaidean sedimentation associated with the development of the Adelaide Rift Complex (Preiss, 2000). Viewed in this context, the metamorphic pressures recorded in the Delamerian-aged mineral assemblages can be used to make inferences about the thickness of the Adelaidean sequences.

Previously, it has been thought that the bulk of the Curnamona Province was only thinly covered by Adelaidean-aged sediments east of the MacDonald Fault (Fig. 11), as this structure was thought to be the eastern limit of deposition in the region during the Neoproterozoic deposition of the Adelaidean sequences (e.g. Preiss, 1987; Preiss, 1993; Paul, 1998; Sandiford et al., 1998; Paul et al., 1999; Preiss, 2000). However this notion is not consistent with recent field mapping by the Department of Primary Industries and Resources South Australia (PIRSA). PIRSA has located regions of Adelaidean outliers infolded as synclinal keels within the Willyama Supergroup, east of the MacDonald Fault (W. Preiss and A. Crooks, pers comm., August 2003; Fig. 11). These include hornblende-bearing calc-sillicates and metasandstones, indicating that in places, Adelaidean sequences have reached upper greenschist to lower amphibolite grade conditions, implying a significant overburden. These observations are supported by the inferred metamorphic pressures from the Kings Dam and Mutooroo Shear Zones, which suggest that around 15 km of overburden must have existed during the Delamerian Orogeny despite limited amounts of shortening. This implies that a thick sequence of Adelaidean rocks covered the southeastern Curnamona Province prior to the Delamerian Orogeny, pointing to the existence of a major half-graben system.

The Weekeroo Inliers offer an excellent opportunity to evaluate the contribution that the cover sequences made to the metamorphism of the basement during the Delamerian Orogeny. In that region the preserved stratigraphic thickness of the Adelaidean cover sequences is 10 to 12 km (Fig. 11; e.g. Preiss, 1987; Preiss, 1993; Paul, 1998), resulting in pressures of around 3.5 kbar. Given that the top of the original sequence conceivably included upper Adelaidean units as well as lateral equivalents of the Kanmantoo Group (Preiss, 2000), there is ample stratigraphic section, combined with modest shortening, to generate the observed metamorphic pressures of 5.0 ± 0.8 kbars from the Walter-Outalpa Shear Zone, which imply around 15 km of burial.

The inference that the regional isograd patterns, in part recorded by the retrograde shear zone assemblages (Fig. 3), largely reflects the pattern of Adelaidean sedimentation has important implications for the mechanics of terrain reactivation during the Delamerian Orogeny. The regions that had undergone the deepest pre-Delamerian burial, also underwent the greatest degree of exhumation, leading to the exposure of ~5 kbar mineral assemblages that formed along thermal gradients of around 35 °Ckm^{-1} (based on the P-T conditions of the Walter-Outalpa Shear Zone). In part the exhumation of these mineral assemblages must have been driven by the compressional Delamerian deformation, suggesting that deformation was most strongly localised in the regions of maximum basement burial, and likely maximum basement temperatures (e.g. Sandiford & Hand, 1998; Hand & Sandiford, 1999). This implies that the pattern and style of terrain reactivation may have been sensitive to the thermal regimes arising from pre-Delamerian processes such as differential accumulation of Adelaidean sequences. This inference is similar to that proposed for other regions in the Australian Proterozoic that appear to have undergone terrain reactivation or reworking largely as a consequence of thermal anomalism linked to pre-orogenic processes such as sedimentation (e.g. Sandiford & Hand, 1998; Sandiford et al., 1998; Hand & Sandiford, 1999; McLaren et al., 2000).

10. Conclusions

Combined metamorphic and geochronological data from greenschist and amphibolite grade mineral assemblages within retrograde shear zones in Palaeoproterozoic basement rocks in the southern Curnamona Province indicate that the peak metamorphic shear zone mineral assemblages formed during the Cambrian Delamerian Orogeny. Peak metamorphic conditions obtained from garnet-staurolite-biotite-muscovite-chlorite-quartz bearing mineral assemblages, which define the shear fabrics, are between 530 and 600°C at ~5 kbars. Garnet zonation patterns indicate that the shear zone assemblages formed during prograde (up-T) mineral growth, indicating that they are unlikely to have formed during post-peak cooling of the 1600-1590 Ma Olarian Orogeny as previously assumed. This is supported by monazite U-Th-Pb and garnet Sm-Nd ages for the shear zone assemblages, which range between 485 to 517Ma. The estimated PT conditions of the Delamerian-aged mineral assemblages have important implications for the inferred PT evolution of the Olarian Orogeny. The currently assumed anticlockwise PT path with isobaric cooling is based largely on the presence of late-stage kyanite formed during the Olarian D_3 event. However, the PT conditions under which shear zones formed during the Delamerian Orogeny are sufficient to stabilise kyanite, and suggest that the late-stage kyanite in the terrain may actually be Delamerian in origin.

The absence of significant up-pressure prograde paths recorded by the shear zone mineral assemblages, and the modest degree of Delamerian-aged shortening suggests that burial was largely a function of Adelaidean sedimentation. Metamorphic pressures obtained from shear zones in the southwestern part of the Curnamona Province suggest that thicknesses of Neoproterozoic Adelaidean sequences were greater 12km. This estimate compares with previous estimates of <4km, and points to the existence of previously unrecognised substantial depocentres that were inverted during the Delamerian Orogeny. The inference that patterns of basement metamorphism and reactivation during the Delamerian Orogeny in part reflects the distribution of pre-Delamerian sedimentation points to the importance of pre-orogenic processes in controlling styles and patterns of terrain reactivation and reworking.

Acknowledgments

I would like to thank my supervisor Martin Hand, Lachlan Rutherford and Karin Barovich for all the help they have given me throughout the year. Jo Mawby for the garnet Sm-Nd analyses and Chris Clark for his assistance with the monazite U-Th-Pb dating. The PIRSA Curnamona team (Wolfgang Preiss, Alistair Crooks and Colin Conor) for their assistance with locations and discussions on isopach maps. Funding for this study has been provided by an Australian Research Council grant to Martin Hand and the Mineral Resources Group of PIRSA.

References

Alias, G., Sandiford, M., Hand, M. and Worley, B., 2002. The P-T record of synchronous magmatism, metamorphism and deformation at Petrel Cove, southern Adelaide Fold Belt. Journal of Metamorphic Geology, 20: 351-363.

Ballevre, M., Le Goff, E. and Hebert, R., 2001. The tectonothermal evolution of the Cadomian Belt of northern Brittany, France; a Neoproterozoic volcanic arc. Tectonophysics, 331(1-2): 19-43.

Becker, H., 1997. Sm-Nd garnet ages and cooling history of high-temperature garnet peridotite massifs and high-pressure granulites from lower-Austria. Contributions to Mineralogy and Petrology, 127: 224-236.

Berry, R.F., Flint, R.B. and Grady, A.E., 1978. Deformation history of the Outalpa area and its application to the Olary Province, South Australia. Transactions of the Royal Society of South Australia, 102: 43-54.

Bierlein, F.P., Foster, D.A. and Plimer, I.R., 1996. Tectonothermal implications of laser $^{40}Ar/^{39}Ar$ ages of sulphide bearing veins and their host rocks in the Willyama Supergroup, South Australia. Mineralogy and Petrology, 58: 1-22.

Bottrill, A.N., 1998. Structural and geochronological analysis of the Walter-Outalpa retrograde shear zone in the eastern Weekeroo inlier. Olary Domain, South Australia. Honours Thesis, University of Adelaide (unpublished).

Burton, K.W., Kohn, B.P., Cohen, A.S. and O'Nions, R.K., 1995. The relative diffusion of Pb, Nd, Sr and O in garnet. Earth and Planetary Science Letters, 133: 199-211.

Butler, C.A., Holdsworth, R.E. and Strachan, R.A., 1995. Evidence for Caledonian sinistral strike-slip motion and associated fault zone weakening, Outer Herbrides Fault Zone, NW Scotland. Journal of the Geological Society, London, 152: 743-746.

Camacho, A. and Fanning, C.M., 1995. Some isotopic constraints on the evolution of the granulite and upper amphibolite facies terranes in the eastern Musgrave Block, central Australia. In: Time limits on tectonic events and crustal evolution using geochronology; some Australian examples. Collins, W.J., Shaw, R.D., (eds) Precambrian Research, 71(1-4): 155-181.

Clarke, G.L., Burg, J.P. and Wilson, C.J.L., 1986. Stratigraphic and structural constraints of the Proterozoic tectonic history of the Olary Block, South Australia. Precambrian Research, 34: 107-137.

Clarke, G.L., Guiraud, M., Powell, R. and Burg, J.P., 1987. Metamorphism in the Olary Block, South Australia: compression with cooling in a Proterozoic fold belt. Journal of Metamorphic Geology, 5: 291-306.

Clarke, G.L., Powell, R. and Vernon, R.H., 1995. Reaction relationships during retrograde metamorphism at Olary, South Australia. Journal of Metamorphic Geology, 13: 715-726.

Clendenin, C.W. and Diehl, S.F., 1999. Structural styles of Paleozoic intracratonic fault reactivation: A case study of the Grays Point fault zone in southeastern Missouri, USA. Tectonophysics, 305: 235-248.

Collins, W.J. and Vernon, R.H., 1991. Orogeny associated with anticlockwise P-T-t paths; evidence from low-P, high-T metamorphic terranes in the Arunta Inlier, central Australia. Geology, 19(8): 835-838.

Conor, C.H.H., 2000. Towards a formal lithostratigraphy for the Olary Domain, Curnamona Province, South Australia. AGSO Record, 2000/10: 23-26.

Cook, N.D.F. and Ashley, P.M., 1992. Meta-evaporite sequence, exhalative chemical sediments and associated rocks in the Proterozoic Willyama Supergroup, South Australia: implications for metallogenesis. Precambrian Research, 56: 211-226.

Corbett, G.J. and Phillips, G.N., 1981. Regional retrograde metamorphism of a high grade terrain: the Willyama Complex, Broken Hill, Australia. Lithos, 14: 59-73.

Dirks, P.H.G.M., Hand, M. and Powell, R., 1991. The P-T deformation path for a mid-Proterozoic, low-pressure terrane; the Reynolds Range, central Australia. Journal of Metamorphic Geology, 9(5): 641-661.

D'Lemos, R.S., Schofield, D.I., Holdsworth, R.E. and King, T.R., 1997. Deep crustal and local rheological controls on the sitting and reactivation of fault and shear zones, northeastern Newfoundland. Journal of the Geological Society, London, 157: 117-121.

Dymoke, P. and Sandiford, M., 1992. Phase relationships in Buchan facies series assemblages: calculations with application to andalusite-staurolite paragenesis in the Mount Lofty Ranges, South Australia. Contributions to Mineralogy and Petrology, 110: 121-132.

Flint, R.B. and Parker, A.J., 1993. Willyama Inliers. In: J.F. Drexel, W.V. Preiss and A.J. Parker (Editors), The Geology of South Australia, Volume 1. The Precambrian. Geological Survey of South Australia Bulletin, pp. 82-93.

Florence, F.P. and Spear, F.S., 1991. Effects of diffusional modification of garnet growth zoning on P-T path calculations. Contributions to Mineralogy and Petrology, 107: 487-500.

Foster, D.A. and John, B.E., 1999. Quantifying tectonic exhumation in an extensional orogen with thermochronology; examples from the southern Basin and Range Province. In: Exhumation processes; normal faulting, ductile flow and erosion. Ring, U., Brandon, M.T., Lister, G.S., Willett, S.D., (eds) Geological Society Special Publications., 154: 343-364.

Glen, R.A., Laing, W.P., Parker, A.J. and Rutland, R.W.R., 1977. Tectonic relationships between the Proterozoic Gawler and Willyama orogenic domains, Australia. Journal of the Geological Society of Australia, 24: 125-150.

Grocott, J., 1977. The relationship between Precambrian Shear belts and modern fault systems. Journal of the Geological Society, London, 133: 257-262.

Hand, M. and Buick, I.S., 2001. Tectonic evolution of the Reynolds-Anmatjira ranges; a case study in terrain reworking from the Arunta Inlier, central Australia. In: Miller, J.A., Holdsworth, R.E., Buick, I.S. & Hand, M. (eds) Continental Reactivation and reworking. Geological Society, London, Special Publications, 184: 237-260.

Hand, M., Rutherford, L. and Barovich, K., 2003. Garnet Sm-Nd age constraints on the timing of tectonism in the southwestern Curnamona Province: Implications for existing models and correlations. In: Peljo, M., comp., 2003. Broken Hill Exploration Initiative: Abstracts from the July 2003 Conference. *Geoscience Australia Record.*, 2003/13: 65-68.

Hand, M. and Sandiford, M., 1999. Intraplate deformation in central Australia, the link between subsidence and fault reactivation. Tectonophysics, 305: 121-140.

Harrison, T.M. and McDougall, I., 1981. Excess ^{40}Ar in metamorphic rocks from Broken Hill, New South Wales: implications for ^{40}Ar/^{39}Ar age spectra and the thermal history of the region. Earth and Planetary Science Letters, 55: 123-149.

Hartley, M.J., Foster, D.A., Gray, D.R. and Kohn, B.P., 1998. 40Ar-39Argon and apatite fission track thermochronology of the Broken Hill Inlier: implications for the Mesoproterozoic to Recent tectonics. AGSO Record, 1998/25: 46-49.

Holdsworth, R.E., Butler, C.A. and Roberts, A.M., 1997. The recognition of reactivation during deformation. Journal of the Geological Society, London, 154: 73-78.

Holdsworth, R.E., Hand, M., Miller, J.A. and Buick, I.S., 2001. Continental reactivation and reworking: an introduction. In: Miller, J.A., Holdsworth, R.E., Buick, I.S. & Hand, M. (eds) Continental Reactivation and reworking. Geological Society, London, Special Publications, 184: 1-12.

Holland, T.J.B. and Powell, R., 1998. An internally consistent dataset for phases of petrological interest. Journal of Metamorphic Geology, 16: 309-343.

Hopwood, T.P., 1993. Geology and ore potential of the Pinnacles Pb-Ag-Zn deposit, Broken Hill, NSW. Report prepared for Pasminco Exploration Limited Consultant's report., No. 123: 1-51.

Imber, J., Holdsworth, R.E., Butler, C.A. and Lloyd, G.E., 1997. Fault-zone weakening processes along the reactivated Outer Hebrides fault zone, Scotland. In: Butler, R.W.H., Holdsworth, R.E., Lloyd, G.E. (eds): The role of basement reactivation in continental deformation. Journal of the Geological Society of London. 154 Part 1, 105-109.

Kohn, M.J. and Spear, F.S., 2000. Retrograde net transfer reaction insurance for pressure-temperature estimates. Geology, 28(12): 1127-1130.

Krabbendam, M., 2001. When the Wilson Cycle breaks down: How orogens can produce strong lithosphere and inhibit their future reworking. In: Miller, J.A., Holdsworth, R.E., Buick, I.S. & Hand, M. (eds) Continental reactivation and reworking. Geological Society, London, Special Publications, 184: 57-76.

Kreissig, K., Holzer, L., Frei, R., Villa, I.M., Kramers, J.D., Kroener, A., Smit, C.A., van Reenen, D.D., 2001. Geochronology of the Hout River shear zone and the metamorphism in the southern marginal zone of the Limpopo Belt, Southern Africa. Precambrian Research, 109(1-2): 145-173.

Laing, W.P., 1969. The geology of the Brewery Well area, northern Barrier Rangers, western New South Wales. Honours Thesis, University of Sydney (unpublished).

Laing, W.P., 1977. Structural geology in a critical area adjacent to the Broken Hill orebody. PhD Thesis, Adelaide University (unpublished).

Laing, W.P., 1996. The Diamantina orogen linking the Willyama and Cloncurry Terrains, eastern Australia. In: J. Pongratz and G.J. Davidson (Editors), New developments in Broken Hill Type deposits. Centre for Ore Deposit and Exploration Studies. CODES Special Publications 1, pp. 67-72.

Laing, W.P., Marjoribanks, R.W. and Rutland, R.W.R., 1978. Structure of the Broken Hill mine area and its significance for the genesis of the orebodies. Economic Geology, 73: 1112-1136.

Laing, W.P., Preiss, W.V., Stevens, B.P. and Flint, R.B., 2002. Interpreted solid geology of the Curnamona Province and surrounding Neoproterozoic and Palaeozoic belts. Department of Primary Industries and Resources, South Australia.

Leven, J.H., Finlayson, D.M., Owen, A., Johnstone, D. and Drummond, B.J., 1998. A seismic model of the crust through the Broken Hill Block and Tasman Line. AGSO research Newsletter, 29: 18-20.

Lishmund, S.R., 1982. Non-metallic and tin deposits of the Broken Hill District. NSW Geological Survey Bulletin, 28: 1-176.

Lu, J., Plimer, I.R., Foster, D.A. and Lottermoser, B.G., 1996. Multiple post-orogenic reactivation in the Olary Block, South Australia: evidence from $^{40}Ar/^{39}Ar$ dating of pegmatitic muscovite. International Geology Review, 38: 665-685.

Ludwig, K.R., 2001. Users manual for Isoplot/Ex: a geochronological toolkit for Microsoft excel. Berkeley Geochronology Centre Special Publication No. 1a.

Mahar, E.M., Baker, J.M., Powell, R., Holland, T.J.B. and Howell, N., 1997. The effect of Mn on mineral stability in metapelites. Journal of Metamorphic Geology, 15: 223-238.

Marjoribanks, R.W., Rutland, R.W.R., Glen, R.A. and Laing, W.P., 1980. The structure and tectonic evolution of the Broken Hill region, Australia. Precambrian Research, 13: 209-240.

Marshak, S. and Paulsen, T., 1996. Midcontinent U.S. fault and fold zones: a legacy of Proterozoic intracratonic extensional tectonism? Geology, 24: 151-154.

Mawby, J., Hand, M. and Foden, J., 1999. Sm-Nd evidence for high-grade Ordovician metamorphism in the Arunta Block, central Australia. Journal of Metamorphic Geology, 17: 653-668.

McLaren, S., Sandiford, M., Dunlap, J. and McDougall, I., 2000. Carboniferous tectonism at Mount Painter; the Alice Springs Orogeny moves south. In: C.G. Skilbeck and T.C.T. Hubble (Editors), Understanding Planet Earth; searching for a sustainable future; abstracts of the 15th Australian geological convention. Geological Society of Australia, Sydney, N.S.W., Australia, pp. 323.

Montel, J.M., Foret, S., Veschambre, M., Nicollet, C. and Provost, A., 1996. Electron microprobe dating of monazite. Chemical Geology, 131: 37-53.

Montel, J.M., Kornprobst, J. and Vielzeuf, D., 2000. Preservation of old U-Th-Pb ages in shielded monazite: example from Beni Bousera Hercynian kinzigites (Morocco). Journal of Metamorphic Geology, 18: 335-342.

Morland, R. and Webster, A.E., 1998. Broken Hill lead-zinc-silver deposit. Geology of Australian and Papua New Guinean mineral deposits, 22. Australasian Institute of Mining and Metallurgy, 619-626 pp.

Murphy, J.B., Keppie, J.D. and Nance, R.D., 1999. Fault reactivation within Avalonia: plate margin to continental interior deformation. Tectonophysics, 305: 183-204.

Needham, T. and Morgan, R., 1997. The east Irish sea and adjacent basins: new faults or old? Journal of the Geological Society, London, 154: 145-150.

Page, R.W. and Laing, W.P., 1992. Felsic metavolcanic rocks related to the Broken Hill Pb-Zn-Ag orebody, Australia; geology, depositional age, and timing of high grade metamorphism. Economic Geology, 87: 2138-2168.

Page, R.W., Stevens, B.P., Conor, C.H.H., Preiss, W.V., Crooks, A.F., Robertson, R.S., Gibson, G.M., 2003. SHRIMP U-Pb geochronology in the Curnamona Province: Improving the framework for mineral exploration. In: Peljo M., comp., 2003. Broken Hill Exploration Initiative: Abstracts from the July 2003 conference. *Geoscience Australia Record*, 2003/13: 122-125.

Page, R.W., Stevens, B.P., Gibson, G.M. and Conor, C.H.H., 2000. Geochronology of Willyama Supergroup rocks between Olary and Broken Hill, and comparison to northern Australia. AGSO Record, 2000/10: 72-75.

Parrish, R.R., 1990. U-Pb dating of monazite and its applications to geological problems. Canadian Journal of Earth Sciences, 27(11): 1431-1450.

Pattison, D.R.M., Spear, F.S. and Cheney, J.T., 1999. Polymetamorphic origin of muscovite+cordierite+staurolite+biotite assemblages: implications for the metapelitic petrogenic grid and for PT paths. Journal of Metamorphic Geology, 17: 685-703.

Paul, E., 1998. The geometry and controls on basement-involved deformation in the Adelaide Fold Belt, South Australia. PhD Thesis, University of Adelaide.

Paul, E., Flottmann, T. and Sandiford, M., 1999. Structural geometry and controls on basement-involved deformation in the northern Flinders Ranges, Adelaide Fold Belt, South Australia. Australian Journal of Earth Sciences, 46(3): 343-354.

Philips, G.N. and Wall, V.J., 1981. Evaluation of prograde regional metamorphic conditions: their implications for the heat source and water activity during metamorphism in the Willyama Complex, Broken Hill, Australia. Bulletin de la Societe Francaise de Mineralogie et de Cristallographie, 104: 801-810.

Pidgeon, R.T., 1967. A rubidium-strontium geochronological study of the Willyama Complex, Broken Hill, Australia. Journal of Petrology, 8: 283-324.

Powell, R. and Holland, T.J.B., 1988. An internally consistent dataset with uncertainties and correlations: 3. Applications to geobarometry, worked examples and a computer program. Journal of Metamorphic Geology, 6: 173-204.

Powell, R. and Holland, T.J.B., 1994. Optimal geothermometry in the pelite system, KFMASH (K_2O-FeO-MgO-Al_2O_3-SiO_2-H_2O). American mineralogist, 79: 120-133.

Preiss, W.V., 2000. The Adelaide Geosyncline of South Australia and its significance in Neoproterozoic continental reconstruction. Precambrian Research, 100: 21-63.

Preiss, W.V., 1993. Neoproterozoic. In: J.F. Drexel, W.V. Preiss and A.J. Parker (Editors), The Geology of South Australia, Volume 1. The Precambrian. Geological Survey of South Australia Bulletin, pp. 171-202.

Preiss, W.V., 1987. The Adelaide Geosyncline-late Proterozoic stratigraphy, sedimentation, palaeontology and tectonics. South Australian Geological Survey, Bulletin 53.

Pyle, J.M., Spear, F.S., Wark, D.A., Daniel, C.G. and Storm, L.C., 2003. Contributions to precision and accuracy of chemical ages of monazite., (Submitted to Journal of Structural Geology).

Raetz, M., Krabbendam, M., Donaghy, A.G., 2002. Compilation of U-Pb zircon data from the Willyama Supergroup, Broken Hill region, Australia; evidence for three tectonostratigraphic successions and four magmatic events?. In: Korsch, R.J. (editor). Geodynamics of Australia and its mineral systems; mineral provinces. Australian Journal of Earth Sciences, 49(6); 965-983.

Richards, J.R. and Pidgeon, R.T., 1963. Some age mesurements on micas from Broken Hill, Australia. Journal of the Geological Society of Australia, 10: 243-260.

Robertson, R.S., Preiss, W.V., Crooks, A.F., Hill, P.W. and Sheard, M.J., 1998. Review of the Proterozoic geology and mineral potential of the Curnamona Province in South Australia. AGSO Journal of Australian Geology and Geophysics, 17(3): 169-182.

Rutland, R.W.R. and Etheridge, M.A., 1975. Two high grade schistosities at Broken Hill and their relation to major and minor structures. Journal of the Geological Society of Australia, 22(3): 259-274.

Sandiford, M. and Hand, M., 1998. Controls on the locus of intraplate deformation in central Australia. Earth and Planetary Science Letters, 162: 97-110.

Sandiford, M., Paul, E. and Flottmann, T., 1998. Sedimentary thickness variations and deformation intensity during basin inversion in the Flinders Rangers, South Australia. Journal of Structural Geology, 20(12): 1721-1731.

Scrimgeour, I. and Raith, J.G., 2001. High-grade reworking of Proterozoic granulites during Ordovician intraplate transpression, eastern Arunta Inlier, central Australia. In: Miller, J.A., Holdsworth, R.E., Buick, I.S. & Hand, M. (eds) Continental Reactivation and reworking. Geological Society, London, Special Publications, 184: 261-287.

Shaw, R.D. and Black, L.P., 1991. The history and tectonic implications of the Redbank thrust zone, central Australia, based on structural, metamorphic and Rb-Sr isotopic evidence. Australian Journal of Earth Sciences, 38(3): 307-332.

Shaw, C.A., Karlstrom, K.E., Williams, M.L., Jercinovic, M.J. and McCoy, A.M., 2001. Electron-microprobe monazite dating of ca. 1.71-1.63 Ga and ca. 1.45-1.38 Ga deformation in the Homestake shear zone, Colorado; origin and early evolution of a persistent intracontinental tectonic zone. Geological Society of AmericaBulletin, 29(8): 739-742.

Spear, F.S., 1993. Metamorphic phase equilibria and pressure-temperature-time paths. Monograph series, 1. Mineralogical Society of America, Washington, D.C.

Spear, F.S. and Cheney, J.T., 1989. A petrogenic grid for pelitic schists in the system SiO_2-Al_2O_3-FeO-MgO-K_2O-H_2O. Contributions to Mineralogy and Petrology, 101: 149-164.

Stevens, B.P., 1986. Post-deformational history of the Willyama Supergroup in the Broken Hill Block, N.S.W. Australian Journal of Earth Sciences, 33: 73-98.

Stevens, B.P., and Bradley, G.M., 1993. Lakes Creek 1:25000 Geological Sheet 7134-II-N. Geological Survey of New South Wales.

Streepey, M.M., Johnson, E.L., Mezger, K. and van der Pluijm, B.A., 2001. Early history of the Carthage-Colton shear zone, Grenville Province, Northwest Adirondacks, New York (U.S.A.). Journal of Geology, 109(4): 479-492.

Stuwe, K. and Ehlers, K., 1997. Multiple metamorphic events at Broken Hill, Australia. Evidence from chloritoid-bearing paragenesis in the Nine-Mile Mine region. Journal of Petrology, 38(9): 1167-1186.

Swapp, S.M. and Frost, B.R., 2003. Evidence for high-pressure metamorphism in the granulites of the Broken Hill area. In: Peljo M., comp., 2003. Broken Hill Exploration Initiative: Abstracts from the July 2003 conference. Geoscience Australia Record, 2003/13: 174-175.

Symmes, G.H. and Ferry, J.M., 1992. The effect of whole-rock MnO content on the stability of garnet in pelitic schists during metamorphism. Journal of Metamorphic Geology, 10: 221-237.

Thatcher, W., 1995. Microplate vrs continuum descriptions of active tectonic deformation. Journal of Geophysical Research, 100: 3885-3894.

Vernon, R.H., 1969. Northwestern region: Archaean or lower Proterozoic rocks, the Willyama Complex, Broken Hill area. In : Packham, G.H. (ed). the Geology of New South Wales. Journal of the Geological Society of Australia, 16: 19-55.

Vernon, R.H. and Ransom, D.M., 1971. Retrograde schists of the amphibolite facies at Broken Hill, New South Wales. Journal of the Geological Society of Australia, 18: 267-277.

Warren, R.G., 1983. Granulites and the tectonic evolution of the Arunta Block, In: Sixth Australian geological convention; Lithosphere dynamics and evolution of continental crust. Geological Society of Australia, Sydney, N.S.W., Australia, pp. 59.

White, R.W., Powell, R. and Philips, G.N., 2003. A mineral equilibria study of hydrothermal alteration in mafic greenschist facies rocks at Kalgoorlie, Western Australia. Journal of Metamorphic Geology, 21(5): 455-468.

Williams, M.L. and Jercinovic, M.J., 2002. Microprobe monazite geochronology: putting absolute time into microstructural analysis. Journal of Structural Geology, 24: 1013-1028.

Williams, P.F. and Vernon, R.H., 2001. Origin of a vertical lineation in conjugate transcurrent shear-zones at Broken Hill, Australia. Tectonophysics, 335: 163-182.

Willis, I.L., 1976. Geology of the Allendale-The Paps-Brewery Well area, Broken Hill. NSW Geological Survey Report, GS 1976/406 (unpublished).

Wilson, C.J.L. and Powell, R., 2001. Strain localisation and high-grade metamorphism at Broken Hill, Australia: a view from the Southern Cross area. Tectonophysics, 335: 193-210.

Wilson, C.J.L., Will, T.M., Cayley, R.A. and Chen, S., 1992. Geologic framework and tectonic evolution in Western Victoria, Australia. Tectonophysics, 214(1-4): 93-97.

Figure Captions

Fig. 1: Location and generalised regional geological map of the Curnamona Province.

Fig. 2: Simplified map of the interpreted regional retrograde shear zone system and igneous intrusives of the Curnamona Province hosted by the Palaeoproterzoic metasediments of the Upper and Lower Willyama Supergroup. The interpreted geology is based on outcrop and geophysical data and has been adapted from the interpreted solid geology of the Curnamona Province and surrounding Neoproterozoic and Palaeozoic belts (Laing et al., 2002). Locations chosen for this study are: 1) Walter-Outalpa RSZ. 2) Kings Dam RSZ. 3) Mutooroo RSZ. 4) Pinnacles mine region. 5 and 6) Thackaringa-Pinnacles RSZ. 7) Stephens Creek RSZ.

Fig. 3: Simplified map of the southern Willyama Supergroup showing the distribution of Olarian (~1600 Ma) metamorphic zones and the observed limit of apparently retrograde (Olarian D_3 ~ 1590 Ma) kyanite and staurolite across the province. Shear zones reach middle amphibolite grade conditions in the highest-grade (2 pyroxene and sillimanite and k-feldspar) zones and decrease to greenschist facies in the north and west. (modified from Stevens, 1986; Clarke et al., 1987; Laing, 1996).

Fig. 4: Block diagram of the Pinnacles mine region showing the major shear zones as steeply dipping structures that cut both Olarian-aged F_1 and F_2 folds. Movement along the shear zones is generally south block up (after Hopwood, 1993).

Fig. 5: Representative petrological relationships in retrograde shear zone assemblages from across the southern Curnamona Province. a) Stephens Creek RSZ: Garnet porphyroblasts overgrown by large subhedral staurolite enveloped by a fine-grained muscovite rich shear fabric. b) Mutooroo RSZ: Large garnet porphyroblasts and smaller staurolite prophyroblasts enveloped in a matrix dominated by chlorite with minor muscovite and biotite. Curved inclusion trails (S_i) within the garnet consisting of ilmenite suggest syn-tectonic prophyroblast growth. c) Walter-Outalpa RSZ: Pressure shadows next to garnet prophyroblasts contain coarse-grained quartz, biotite and plagioclase. d) Kings Dam RSZ. Garnet prophyroblast being overgrown by staurolite in a quartz-rich matrix. Late chlorite crystals cross cut the shear fabric. e) Kings Dam RSZ: Garnet prophyroblast over grown by staurolite within a quartz-biotite matrix. Late subhedral staurolite crystals crosscut the shear fabric suggesting post-kinematic growth. f) Thackaringa-Pinnacles RSZ: Large garnet prophyroblast with inclusions of staurolite, ilmenite and orthoamphibole, within a matrix dominated by chlorite and plagioclase.

Fig. 6: Qualatative compositional cation maps (Mg, Fe, Ca and Mn) of garnets from the Mutooroo RSZ. Note the increase of Mg and Fe towards the rim and the distinct

rimward decrease of Mn, which is indicative of prograde growth zonation (lighter areas indicate higher concentrations with darker areas being lower concentrations).

Fig. 7: a) Plot of pressure against XH_2O (mole fraction of H_2O in a H_2O-CO_2 fluid) at a temperature of 525 °C. Note that as the XH_2O decreases, the pressure increases. The calculated pressures are within 95% confidence when the fit value is below 1.37. b) Plot of temperature against XH_2O at a pressure of 5 kbar. Note that temperature decreases with decreasing XH_2O. The calculated temperatures are within 95% confidence when the fit value is below 1.43.

Fig. 8: a) Backscatter image of a typical monazite from within the matrix fabric of the Stephens Creek RSZ. b, c and d) plots of monazite geochronology analyses showing the weighted average age, MSWD and the error (vertical Axis) for each data point analysed (horizontal axis).

Fig. 9: PT pseudosection of Stuwe and Ehlers (1997) in the system KFMASH +quartz +H_2O. This pseudosection was constructed to model amphibolite-grade mineral assemblages in the Nine Mile Creek region north of Broken Hill, and can be effectively used to portray the petrological evolution of selected retrograde shear zones (see text for details). PT ellipse for the Walter-Outalpa RSZ is indicated showing the PT conditions of shear zone formation. Arrows indicate the inferred

general path of rocks from the Thackaringa-Pinnacles (up PT arrow) and the Kings Dam (down PT arrow) RSZ.

Fig. 10: PT pseudosection of Mahar et al. (1997) in the system MnKFMASH +muscovite +quartz+ H_2O, which is applicable to selected MnO-bearing shear zone assemblages. The PT ellipse for the Walter-Outalpa RSZ is shown indicating the general PT conditions of formation for the RSZ's. The arrow indicates the general path of group 1 shear zone assemblages (see sect. 4).

Fig. 11: Isopach map of the inferred thickness of Neoproterozoic Adelaidean cover over the Palaeoproterozoic Willyama Supergroup prior to the Delamerian Orogeny (~500Ma; compiled from Preiss 1987; Preiss, 1993; Paul, 1998; Paul et al., 1999; intervals at 1 km). Locations of Amphibolite bearing Adelaidean metasediments indicate isopachs are incorrect and that the region was subjected to greater amounts of burial. Metamorphic isograds for staurolite in and kyanite in may indicate currently unobserved Adelaidean depocentres.

Figure 1

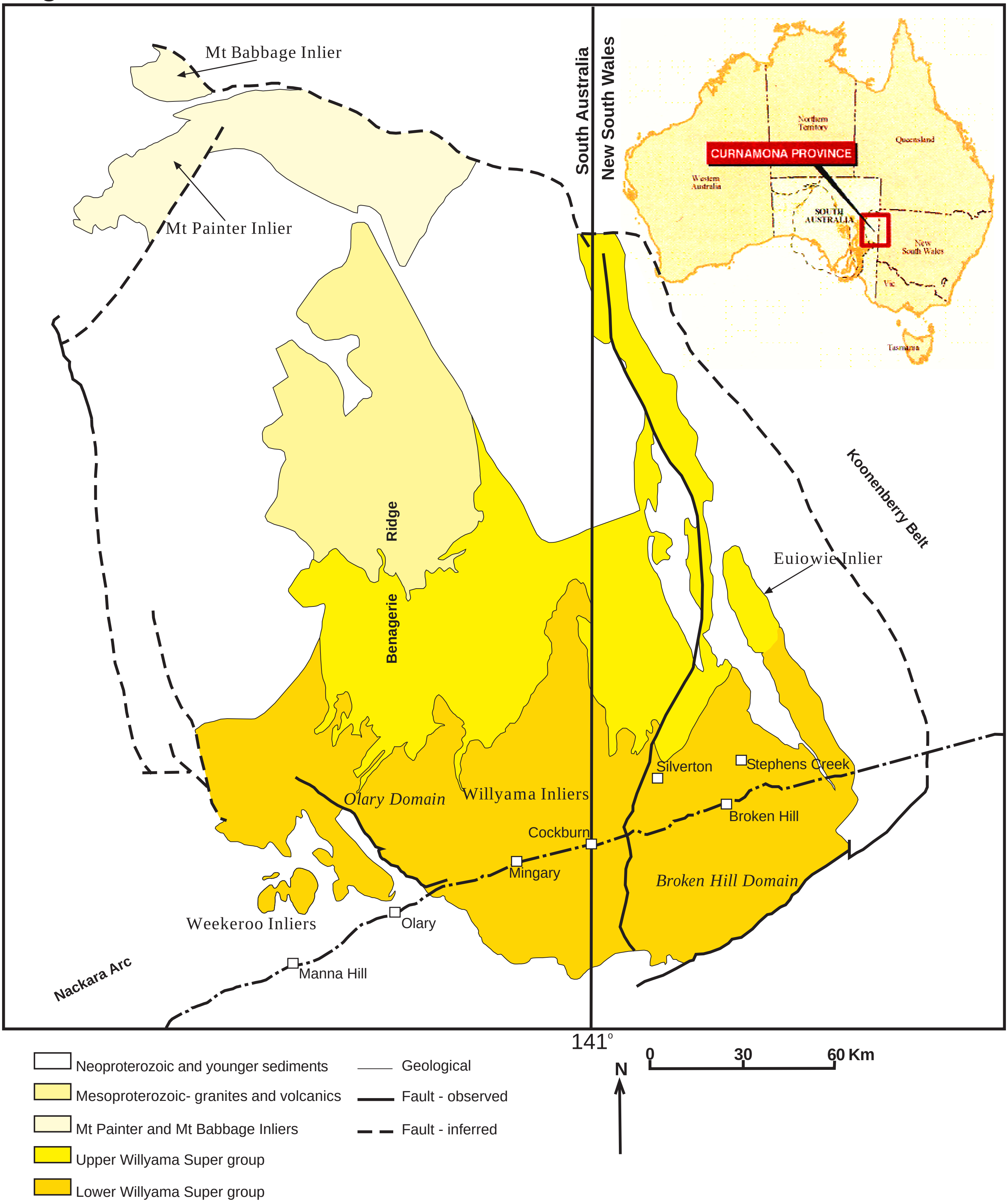

Mt Babbage Inlier
Mt Painter Inlier
South Australia
New South Wales
CURNAMONA PROVINCE
Northern Territory
Queensland
Western Australia
SOUTH AUSTRALIA
New South Wales
Vic
Tasmania
Koonenberry Belt
Euiowie Inlier
Benagerie Ridge
Silverton
Stephens Creek
Broken Hill
Olary Domain
Willyama Inliers
Cockburn
Mingary
Broken Hill Domain
Weekeroo Inliers
Olary
Manna Hill
Nackara Arc
141°
N
0
30
60 Km
Neoproterozoic and younger sediments
Mesoproterozoic- granites and volcanics
Mt Painter and Mt Babbage Inliers
Upper Willyama Super group
Lower Willyama Super group
Geological
Fault - observed
Fault - inferred

Figure 2

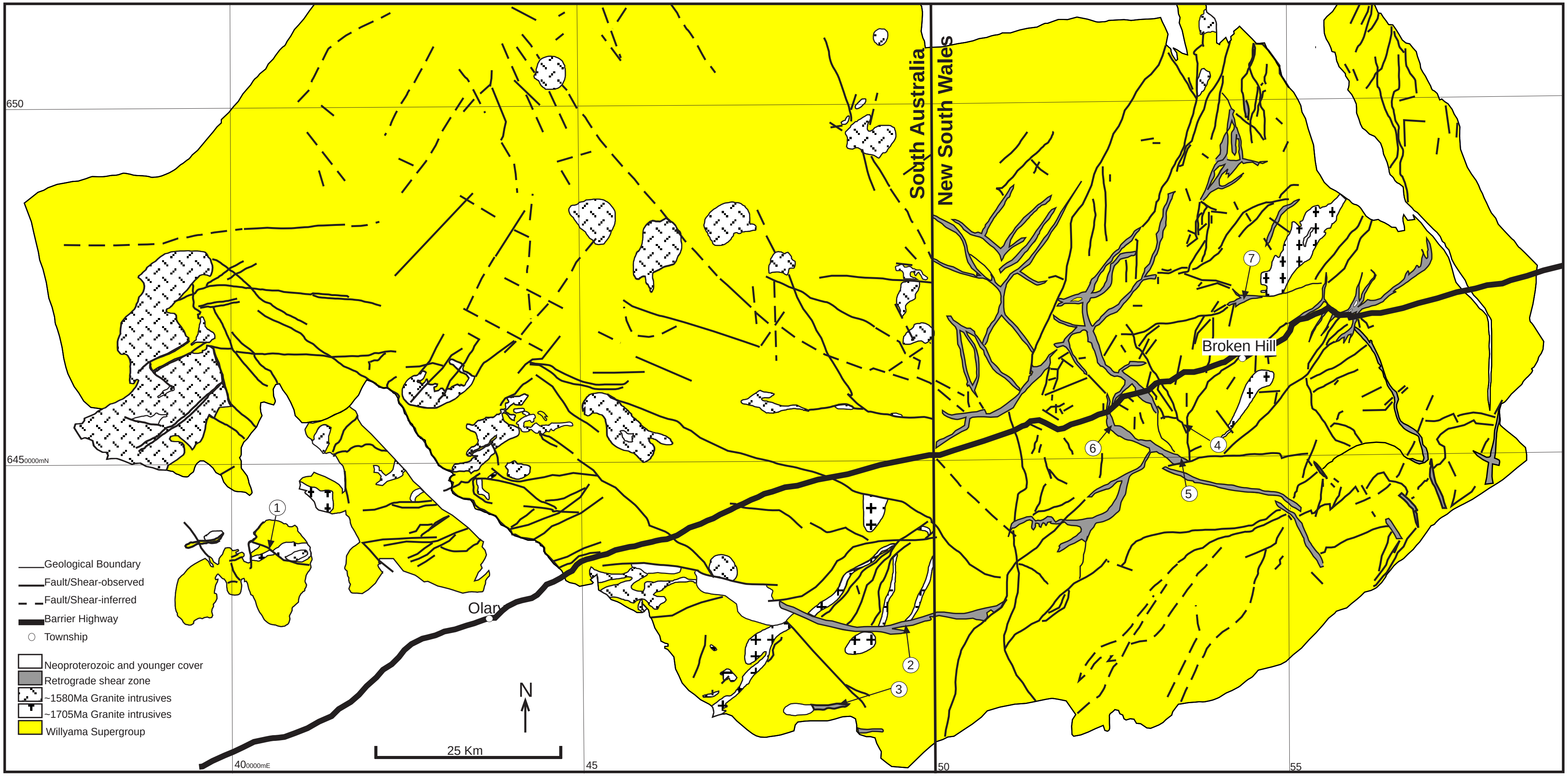

South Australia
New South Wales
Broken Hill
Olary
650
645 0000mN
40 0000mE
45
50
55
25 Km
N
1
2
3
4
5
6
7
Geological Boundary
Fault/Shear-observed
Fault/Shear-inferred
Barrier Highway
Township
Neoproterozoic and younger cover
Retrograde shear zone
~1580Ma Granite intrusives
~1705Ma Granite intrusives
Willyama Supergroup

Figure 3

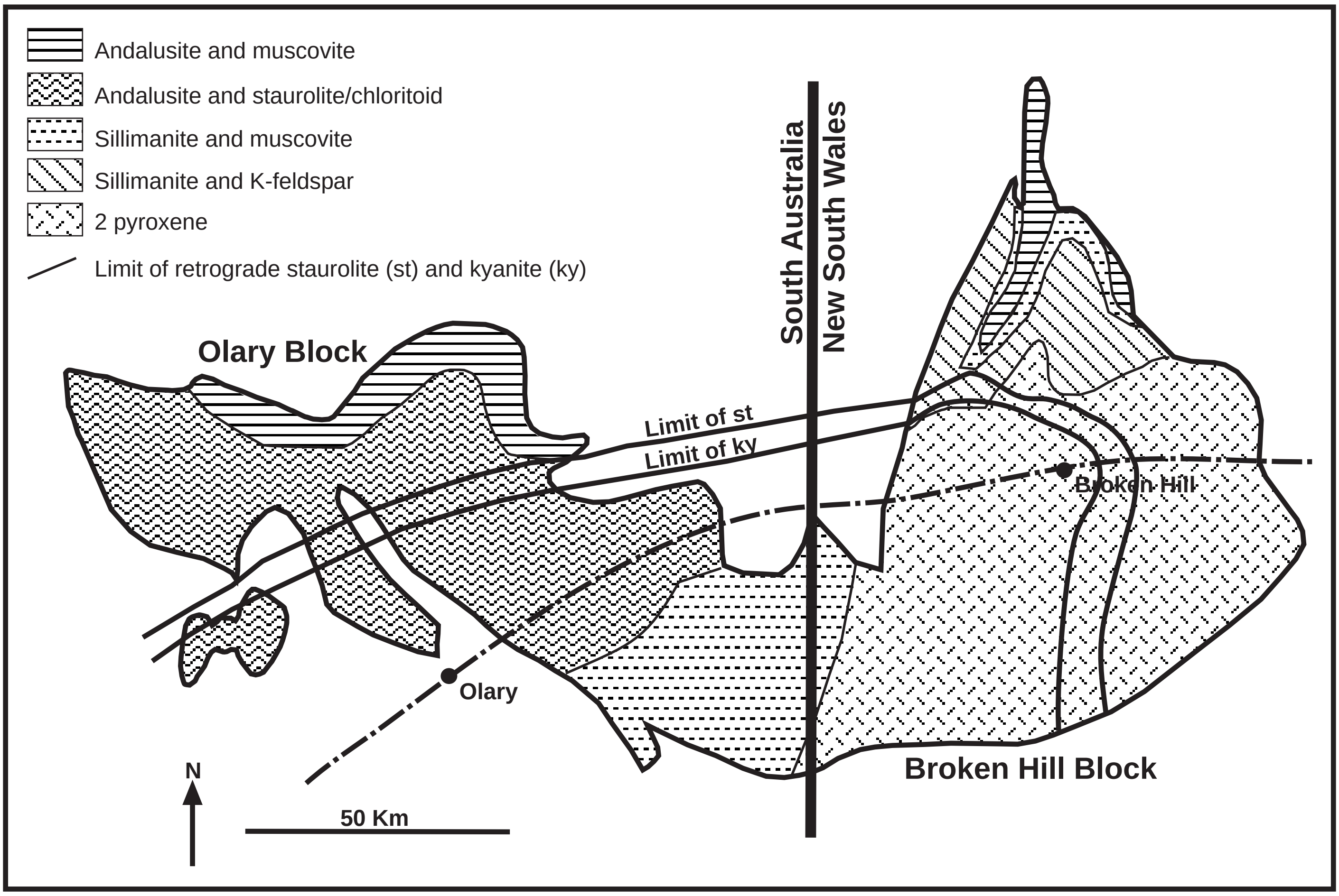

Andalusite and muscovite
Andalusite and staurolite/chloritoid
Sillimanite and muscovite
Sillimanite and K-feldspar
2 pyroxene
Limit of retrograde staurolite (st) and kyanite (ky)
South Australia
New South Wales
Olary Block
Limit of st
Limit of ky
Broken Hill
Olary
Broken Hill Block
N
50 Km

Figure 4

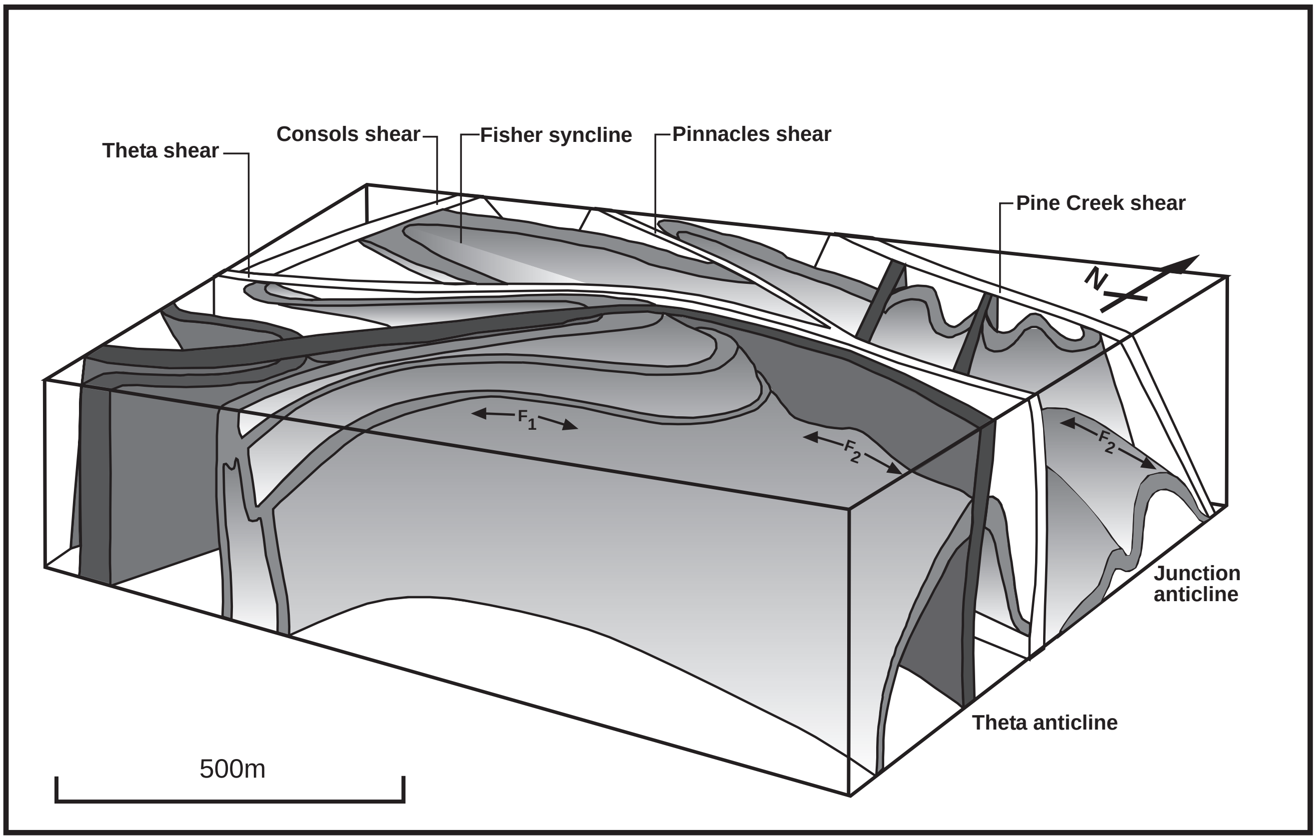

Theta shear
Consols shear
Fisher syncline
Pinnacles shear
Pine Creek shear
N
F1
F2
F2
Junction anticline
Theta anticline
500m

Figure 5

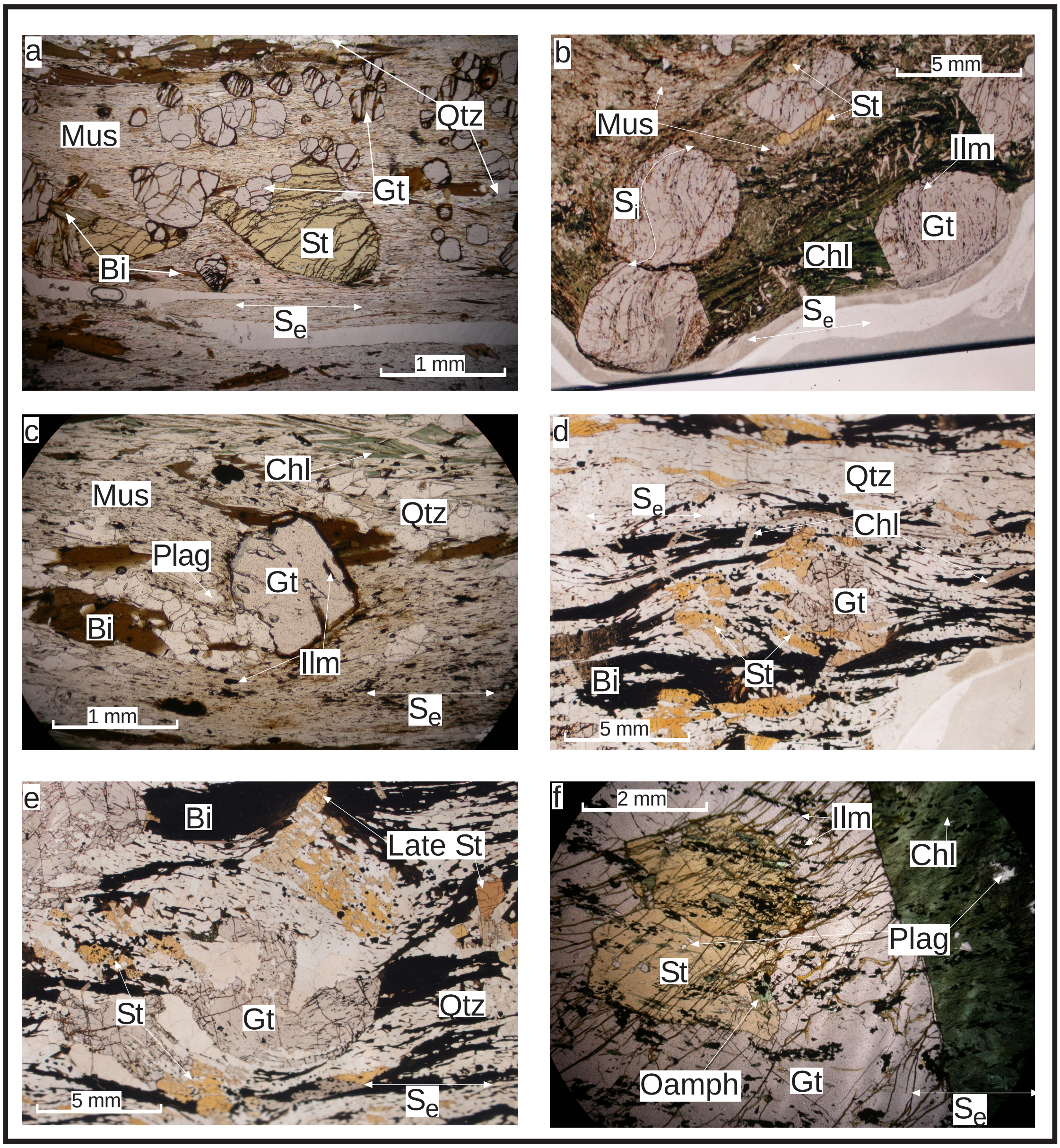

a
Qtz
Mus
Gt
St
Bi
S_e
1 mm
b
5 mm
St
Mus
Ilm
S_i
Gt
Chl
S_e
c
Chl
Mus
Qtz
Plag
Gt
Bi
Ilm
1 mm
S_e
d
Qtz
S_e
Chl
Gt
St
Bi
5 mm
e
Bi
Late St
St
Gt
Qtz
5 mm
S_e
f
2 mm
Ilm
Chl
Plag
St
Oamph
Gt
S_e

Figure 6

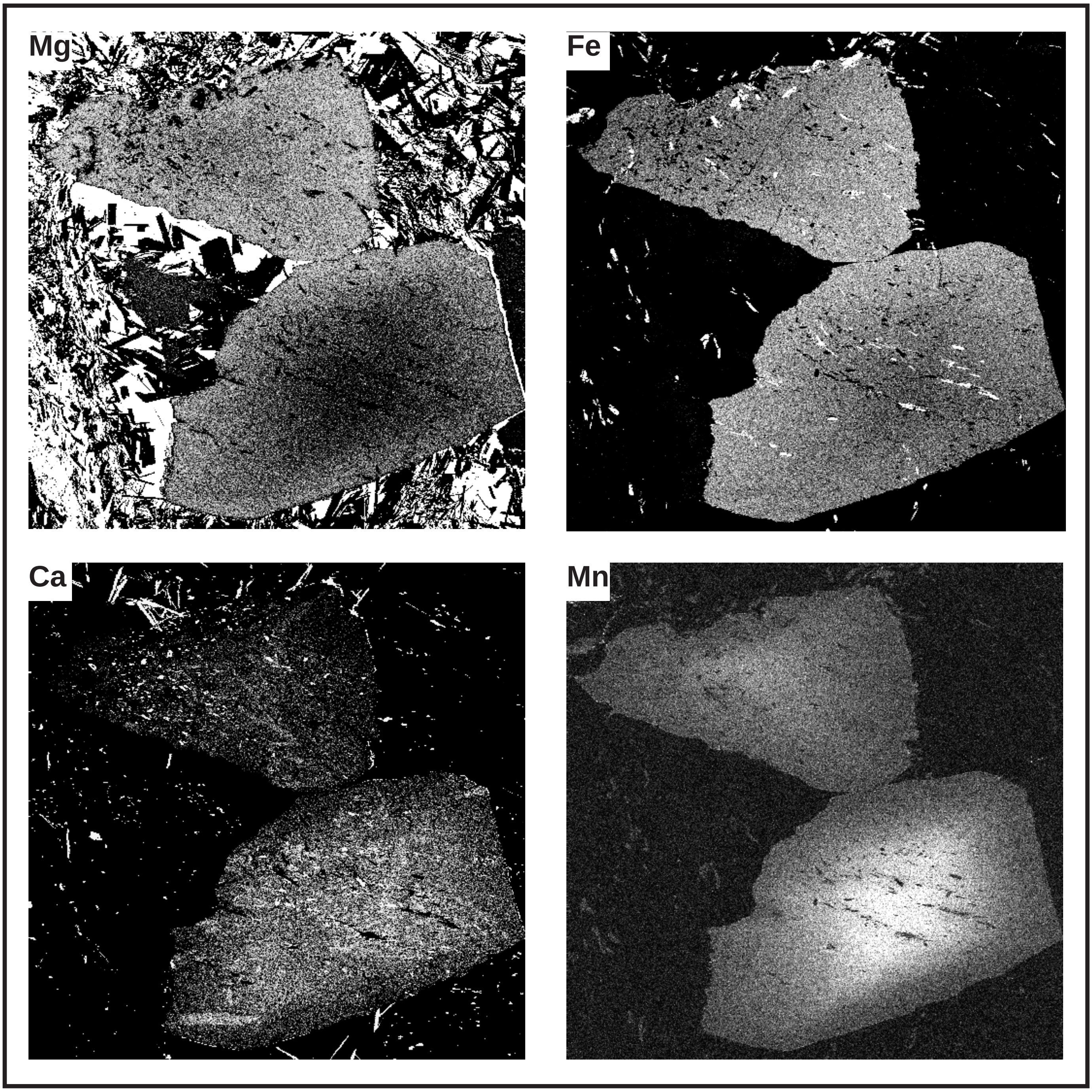

Figure 7

a

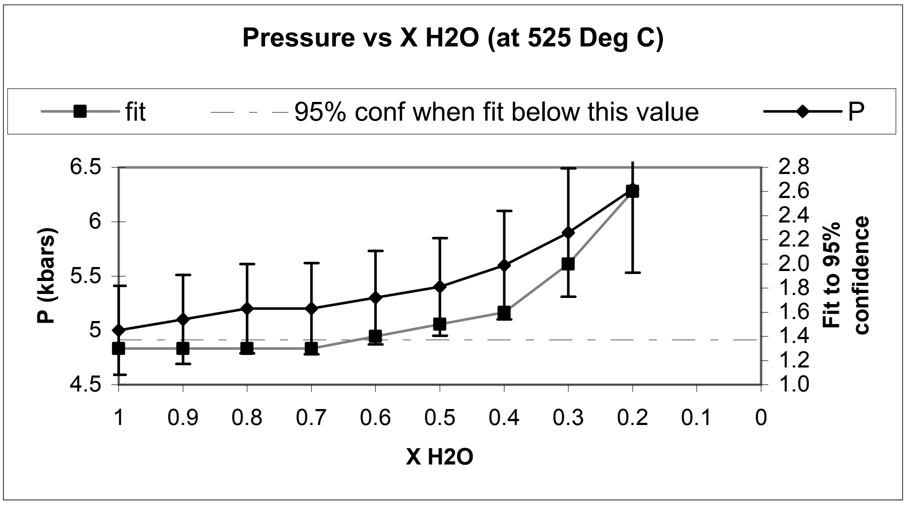

Pressure vs X H2O (at 525 Deg C)
fit
95% conf when fit below this value
P
P (kbars)
Fit to 95% confidence
X H2O
6.5
6
5.5
5
4.5
2.8
2.6
2.4
2.2
2.0
1.8
1.6
1.4
1.2
1.0
1
0.9
0.8
0.7
0.6
0.5
0.4
0.3
0.2
0.1
0

b

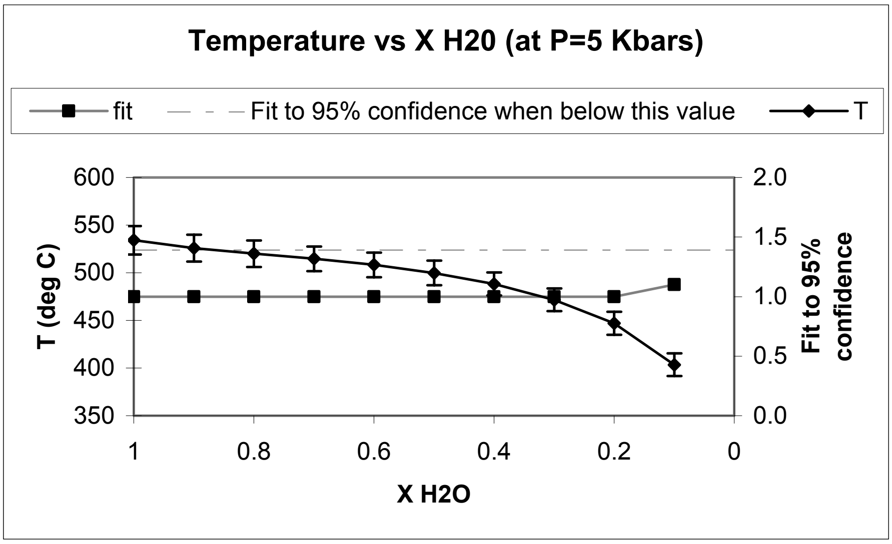

Temperature vs X H20 (at P=5 Kbars)
fit
Fit to 95% confidence when below this value
T
T (deg C)
Fit to 95% confidence
X H2O
600
550
500
450
400
350
2.0
1.5
1.0
0.5
0.0
1
0.8
0.6
0.4
0.2
0

Figure 8

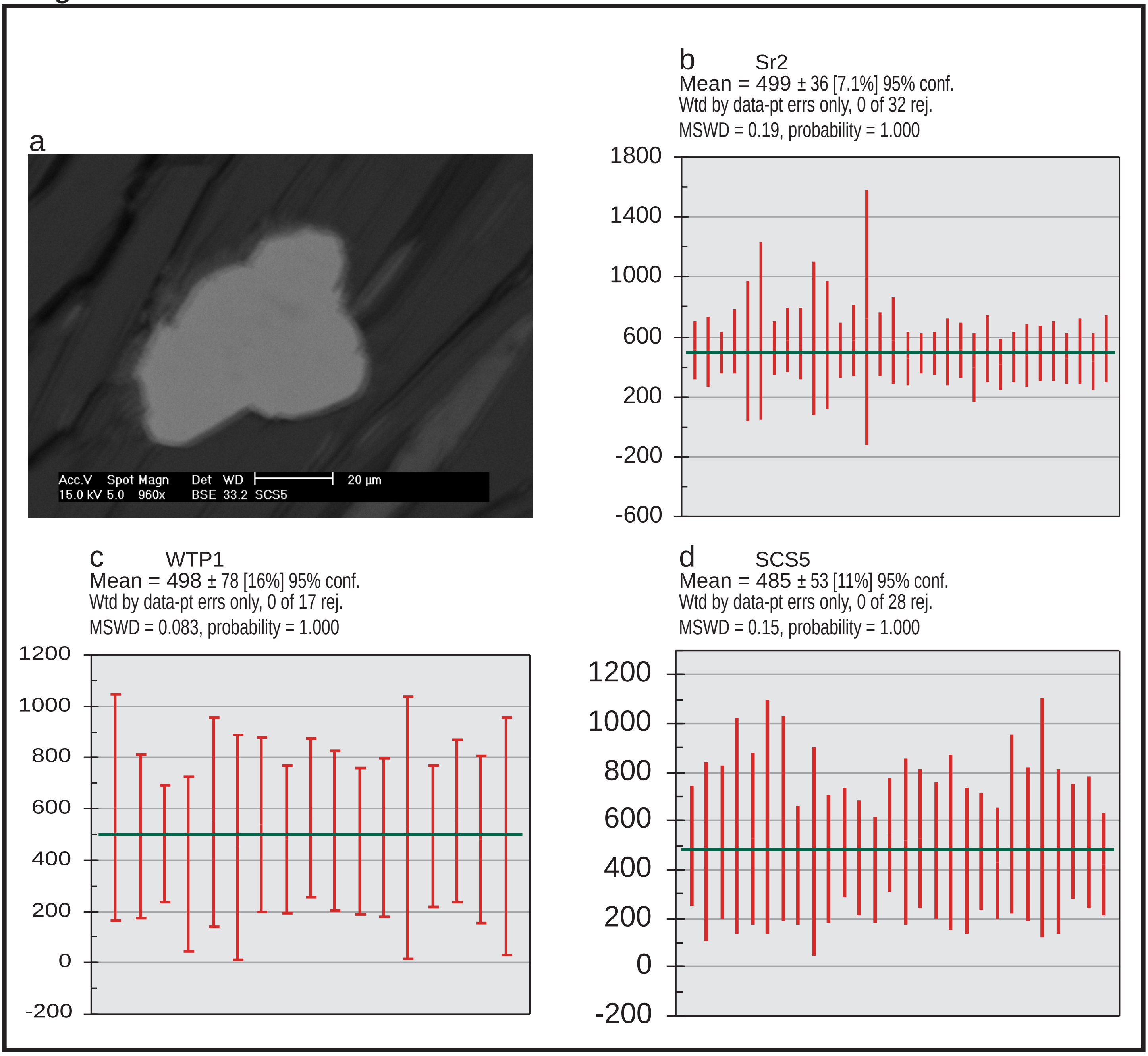
a
Acc.V Spot Magn Det WD 20 µm
15.0 kV 5.0 960x BSE 33.2 SCS5
b Sr2
Mean = 499 ± 36 [7.1%] 95% conf.
Wtd by data-pt errs only, 0 of 32 rej.
MSWD = 0.19, probability = 1.000
1800
1400
1000
600
200
-200
-600
c WTP1
Mean = 498 ± 78 [16%] 95% conf.
Wtd by data-pt errs only, 0 of 17 rej.
MSWD = 0.083, probability = 1.000
1200
1000
800
600
400
200
0
-200
d SCS5
Mean = 485 ± 53 [11%] 95% conf.
Wtd by data-pt errs only, 0 of 28 rej.
MSWD = 0.15, probability = 1.000
1200
1000
800
600
400
200
0
-200

Figure 9

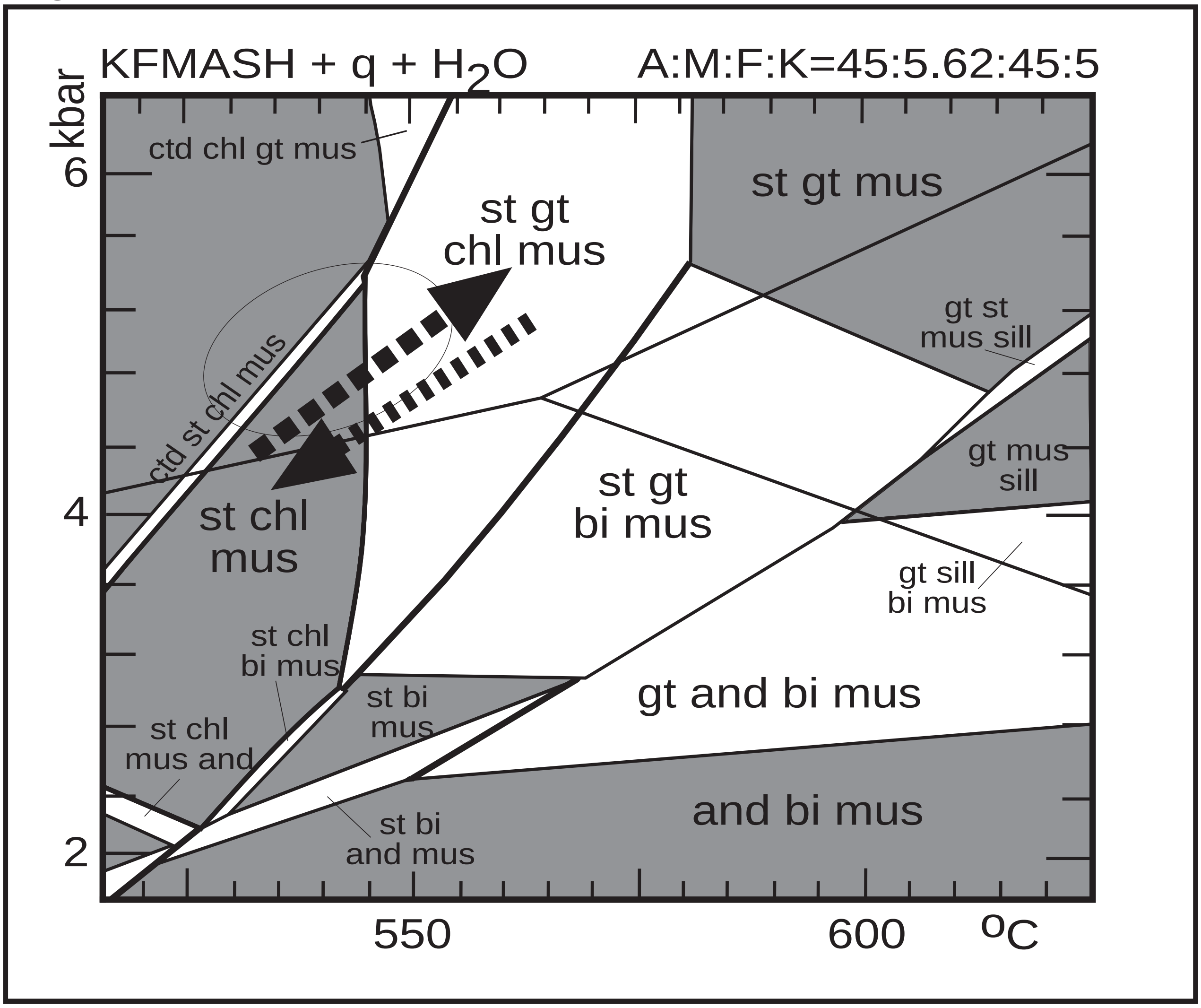

KFMASH + q + H2O
A:M:F:K=45:5.62:45:5
kbar
6
4
2
550
600
oC
ctd chl gt mus
st gt
chl mus
st gt mus
gt st
mus sill
ctd st chl mus
st chl
mus
st gt
bi mus
gt mus
sill
gt sill
bi mus
st chl
bi mus
st bi
mus
st chl
mus and
gt and bi mus
and bi mus
st bi
and mus

Figure 10

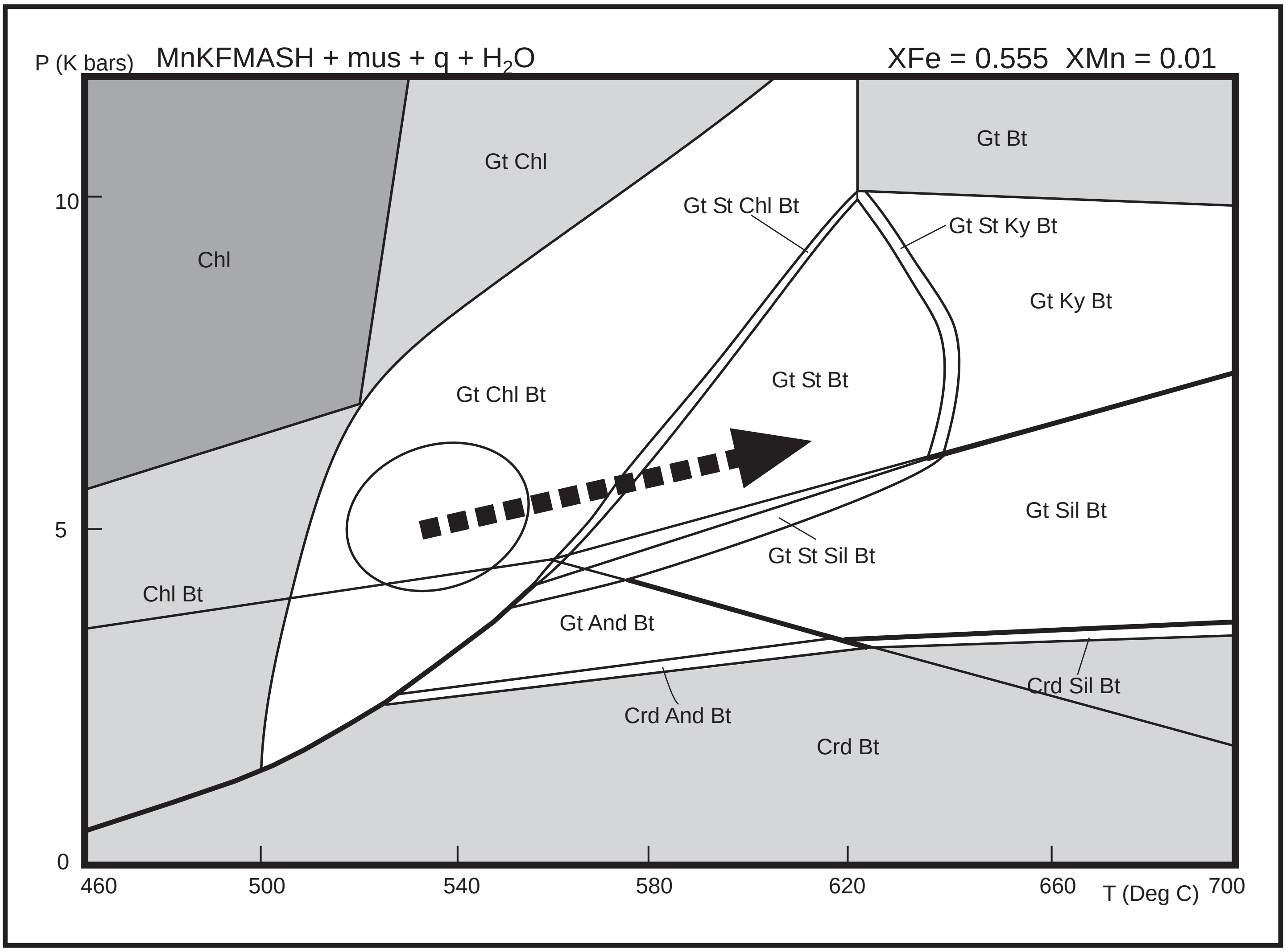

P (K bars)
MnKFMASH + mus + q + H_2O
XFe = 0.555 XMn = 0.01
Gt Bt
Gt Chl
Gt St Chl Bt
Gt St Ky Bt
Chl
Gt Ky Bt
Gt St Bt
Gt Chl Bt
Gt Sil Bt
Gt St Sil Bt
Chl Bt
Gt And Bt
Crd Sil Bt
Crd And Bt
Crd Bt
10
5
0
460
500
540
580
620
660
700
T (Deg C)

Figure 11

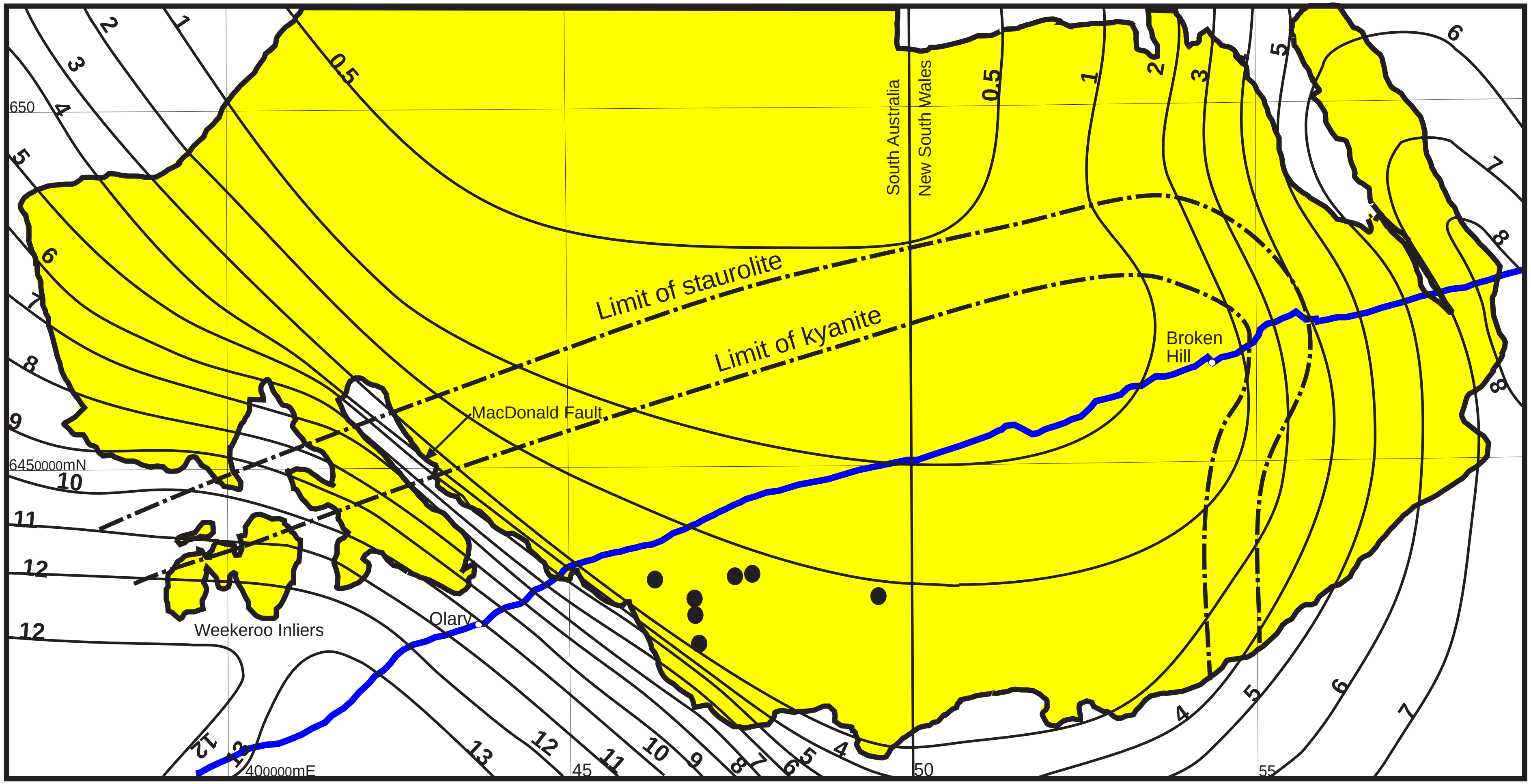

Geological Boundary

Thickness of Cover Sequences in km

Barrier Highway

○ Township

● Locations of amphibolite grade Adelaidean

Metamorphic isograds for kyanite and staurolite out

Neoproterozoic and younger cover

Willyama Supergroup

25 Km

N

Table 1: Representative mineral compositions

Sample	RD-11	RD-11	RD-11	KD1b-st1	KD1b-st2	KD1b-st3	RD8-1	Rd8-2	RD11-2	RD11-1	RD11-2	RD11-3	RD8-3
Mineral	ep	ep	ep	st	st	st	gt rim	gt rim	gt rim	gt core	gt core	gt core	mus
SiO2	37.870	37.370	37.330	25.700	27.270	27.150	35.690	35.310	36.430	36.12	35.86	36.5	47.410
TiO2	0.170	0.000	0.080	0.540	0.490	0.270	0.000	0.030	0.000	0.1	0.18	0.12	0.240
Al2O3	24.460	24.320	24.060	52.350	54.760	53.900	19.980	19.780	19.950	19.67	20	19.8	33.600
Cr2O3	0.000	0.010	0.040	0.000	0.000	0.030	0.000	0.060	0.010	0.07	0.03	0.03	0.100
Fe2O3	12.330	12.400	12.020	0.000	0.000	0.000	3.820	5.330	1.930	3.26	3.55	2.85	0.000
FeO	0.110	0.110	0.110	16.910	16.930	17.020	22.540	21.260	21.330	12.6	15.14	14.56	3.670
MnO	0.210	1.120	1.180	0.040	0.000	0.010	14.790	15.120	14.710	21.72	20.2	21.27	0.100
MgO	0.020	0.010	0.000	1.440	1.240	1.440	1.640	1.530	1.610	0.6	0.75	0.66	0.940
CaO	20.040	21.380	21.150	0.020	0.000	0.000	1.560	1.650	3.310	5.39	4.58	4.64	0.140
Na2O	0.030	0.130	0.010	0.000	0.040	0.000	0.050	0.080	0.030	0.13	0.04	0.07	1.070
K2O	0.010	0.040	0.000	0.000	0.000	0.010	0.000	0.160	0.020	0.03	0.01	0.07	12.100
Totals	95.250	96.900	95.990	96.990	100.730	99.830	100.070	100.290	99.340	99.69	100.33	100.55	99.380
Oxygens	12.5	12.5	12.5	46.0	46.0	46.0	12.0	12.0	12.0	12.0	12.0	12.0	11.0
Si	3.055	2.996	3.016	7.338	7.461	7.502	2.922	2.892	2.981	2.955	2.923	2.965	3.101
Ti	0.010	0.000	0.005	0.115	0.101	0.056	0.000	0.002	0.000	0.006	0.011	0.007	0.012
Al	2.326	2.299	2.292	17.620	17.660	17.560	1.929	1.909	1.925	1.897	1.921	1.897	2.591
Cr	0.000	0.001	0.003	0.000	0.000	0.006	0.000	0.004	0.001	0.004	0.002	0.002	0.005
Fe3	0.748	0.748	0.731	0.000	0.000	0.000	0.235	0.328	0.119	0.201	0.217	0.174	0.000
Fe2	0.008	0.008	0.007	4.037	3.872	3.933	1.543	1.456	1.460	0.862	1.032	0.989	0.201
Mn	0.014	0.076	0.081	0.009	0.000	0.003	1.026	1.049	1.020	1.505	1.394	1.464	0.006
Mg	0.002	0.002	0.000	0.611	0.504	0.594	0.200	0.187	0.197	0.074	0.091	0.08	0.091
Ca	1.732	1.837	1.831	0.007	0.000	0.000	0.137	0.144	0.291	0.473	0.4	0.404	0.010
Na	0.005	0.020	0.002	0.000	0.020	0.002	0.008	0.013	0.005	0.021	0.007	0.011	0.135
K	0.001	0.004	0.000	0.000	0.000	0.003	0.000	0.016	0.002	0.003	0.002	0.007	1.011
Sum	7.901	7.992	7.968	29.737	29.618	29.660	8.000	8.000	8.000	8.000	8.000	8.000	7.162

Table 1: Representative mineral compositions *(continued)*

RD11-1	RD11-2	RD8-2	RD8-3	RD11-2	RD8-1	RD8-2	RD11-3	RD8-1	RD8-2	RD8-3
mus	mus	bi	bi	bi	plag	plag	plag	chl	chl	chl
48.160	48.260	33.890	34.870	34.690	60.090	59.530	59.160	24.390	22.770	23.560
0.300	0.430	1.760	1.560	2.110	0.060	0.010	0.060	0.030	0.110	0.060
33.790	34.850	18.530	19.470	18.900	24.950	25.380	23.320	21.820	20.580	21.660
0.000	0.030	0.000	0.000	0.040	0.000	0.000	0.000	0.000	0.010	0.020
0.000	0.000	2.990	1.540	0.400	0.170	0.320	0.430	2.260	3.830	4.300
3.870	3.190	24.450	25.810	24.890	0.000	0.000	0.000	26.120	23.150	23.280
0.010	0.000	0.040	0.000	0.070	0.000	0.080	0.060	0.370	0.420	0.480
0.900	0.720	7.490	7.120	7.570	0.010	0.000	0.000	14.290	14.190	14.940
0.100	0.120	0.000	0.020	0.010	6.200	7.320	5.330	0.020	0.050	0.010
0.840	0.890	0.510	0.470	0.500	7.330	7.470	8.750	0.000	0.010	0.070
11.230	11.910	9.860	9.880	9.450	0.110	0.090	0.070	0.000	0.040	0.050
99.220	100.410	99.530	100.750	98.630	98.920	100.210	97.190	89.300	85.160	88.430
11.0	11.0	11.0	11.0	11.0	8.0	8.0	8.0	14.0	14.0	14.0
3.131	3.101	2.571	2.605	2.629	2.694	2.653	2.713	2.559	2.503	2.486
0.014	0.021	0.101	0.088	0.120	0.002	0.000	0.002	0.003	0.009	0.005
2.590	2.640	1.657	1.715	1.689	1.319	1.333	1.261	2.699	2.666	2.695
0.000	0.001	0.000	0.000	0.002	0.000	0.000	0.000	0.000	0.001	0.002
0.000	0.000	0.171	0.087	0.023	0.006	0.011	0.015	0.178	0.317	0.342
0.211	0.171	1.552	1.613	1.577	0.000	0.000	0.000	2.292	2.128	2.055
0.001	0.000	0.003	0.000	0.004	0.000	0.003	0.002	0.033	0.039	0.043
0.087	0.069	0.847	0.792	0.855	0.000	0.000	0.000	2.235	2.325	2.350
0.007	0.009	0.000	0.001	0.001	0.298	0.350	0.262	0.002	0.006	0.002
0.106	0.110	0.075	0.068	0.073	0.637	0.645	0.778	0.000	0.001	0.014
0.933	0.978	0.955	0.942	0.914	0.006	0.005	0.004	0.000	0.006	0.007
7.079	7.101	7.930	7.911	7.887	4.963	5.000	5.038	10.000	10.000	10.000

Table 2: P-T conditions of shear zone formation

Shear zone	Sample Number	T °C (1σ)	P Kbars	T °C (ave) At 2σ
Walter-Outalpa	RD11-1 RD11-2 RD15-1 RD15-2 RD8-1 RD8-2	528 ± 11 533 ± 14 525 ± 15 544 ± 90 511 ± 14 564 ± 16	5 ± 0.82 (2σ)	534 ± 20
Kings Dam	KD-1 KD-2 KD-1b	598 ± 49 617 ± 95 567 ± 14		594 ± 60
Mutooroo	Ma-1	563 ± 14		563 ± 28
Thackaringa-Pinnacles	Sr-1 Tp-1 WTP1	570 ± 97 595 ± 13 540 ± 99		568 ± 80
Stephens Creek	SCS5-1 SCS5-2 SCS5-3	570 ± 15 550 ± 10 559 ± 14		559 ± 15

Table 3: Garnet Sm-Nd and Monazite U-Th-Pb ages for sampled shear zones		
Shear zone	Garnet Sm-Nd Age (Ma)	Monazite U-Th-Pb Age (Ma)
Kings Dam	503 ± 13	-
Mutooroo	517 ± 14	-
Thackaringa-Pinnacles	500 ± 10	499 ± 36 (n = 32) 498 ± 78 (n = 17)
Stephens Creek	-	485 ± 53 (n = 28)

Table 4: Representative monazite compositions

Label	SCS5_2	SCS5_4	SCS5_6	SR2_1	SR2_2	SR2_3	WTP1_1	WTP1_2	WTP1_3	Standard
W%(O)	25.3014	25.9016	26.2539	26.0223	26.0229	25.9251	25.441	25.7549	25.3959	25.1471
W%(Al)	0.0327	0.0325	0.012	0.0037	0.0013	0.0113	0.0154	0.0021	0.0181	0.0025
W%(Si)	0.4752	0.4254	0.2188	0.4886	0.3267	0.105	0.1653	0.1221	0.1709	0.7041
W%(P)	11.4889	11.9596	12.4898	11.9232	12.1062	12.2617	11.7048	12.0474	11.6689	11.0186
W%(Ca)	1.02	0.9219	0.6445	1.3957	1.022	1.6882	0.7571	0.6937	0.9653	0.2965
W%(Y)	1.0487	1.0475	1.045	1.0539	0.8944	0.9524	0.5375	0.706	0.5827	0.6132
W%(La)	10.7094	10.9197	11.815	9.7622	9.1825	10.2746	11.9637	12.1394	11.6207	11.3368
W%(Ce)	23.8481	24.7249	26.1606	23.3166	24.7429	23.0945	26.8824	26.9324	25.994	27.5751
W%(Pr)	2.2221	2.2068	2.3475	2.2045	2.452	2.0829	2.4835	2.4204	2.4392	2.5500
W%(Nd)	8.5787	8.797	9.0146	8.2537	10.5937	7.9288	9.2021	9.3906	9.1495	8.9355
W%(Sm)	1.4318	1.5178	1.4797	1.3041	1.7559	1.276	1.5684	1.5181	1.4216	1.7112
W%(Gd)	1.24	1.2909	1.3794	1.1834	1.1946	1.1192	1.162	1.2345	1.1721	0.8557
W%(Dy)	0.5569	0.5107	0.5293	0.5408	0.4655	0.3748	0.4141	0.3652	0.4082	0.2388
W%(Er)	0.0587	0.0578	0.1336	0.0993	0.1017	0.1103	0.1119	0.1658	0.0406	0.0885
W%(Pb)	0.1798	0.2013	0.1203	0.3027	0.221	0.4122	0.1721	0.1498	0.1905	0.1641
W%(Th)	8.556	7.4833	4.3455	10.9657	6.8538	6.9496	4.5724	3.3526	5.1747	6.5261
W%(U)	0.3368	0.3362	0.2549	0.4566	0.7148	3.3285	0.3584	0.8396	0.9957	0.2166
Totals	97.0852	98.3349	98.2444	99.277	98.6519	97.8951	97.5121	97.8346	97.4086	97.9802

Appendix 1: Sample locations, group numbers and descriptions

Location		**Group**	**Sample**	**Description**	**SZ Orientation**	**Mineralogy**
0404743	6438506	1	RD5-RD15	gt-chl schist zone	090/81 S top to N	Gt, Cl, Mus shist +/- Tormaline
Walter oultalpa sz					Lx 78->N	
491952	6426563	2	Kd1	no outcrop	E-W steeply dipping	Coarse grained mus+bi+qtz+large gt+st
Kings Dam sz						
491272	6411714	1	Ma 1	no outcrop	NW-SE steeply dipping	quartz poor gt+st+bi chlorite shist
Mutooroo sz						
0531487	6454141	1	P1-3	Gt + Bi alteration zone on the		Wethered Gt sericite shist+ St-Sericite shist
Pinnacles mine area				margin of the Pinnacles lode		Gt-St-sericite shist
				horizon		St-Sericite shist
0531711	6454466		P4	Gt bearing Amphibolite. Dosnt	160/75 W	Gt-Hnbd Amphibolite
				look granulite grade/amphib		
				flanked by retro shear		
Pinnacles Mine Core		1	PN 1+2	DD core PN82W-109.4m		Gt+Chl+ Bi+ sericite shist
			PN 3+8	DD core PN82W-52.5m		Gt+Chl+ Bi+ sericite shist
			PN 4+7	DD core PN73W-134.7m		Gt+Chl+ Bi+ sericite shist
			PN 5+6	DD core PN 51W-216.8m		Gt+Chl+ Bi+ sericite shist
0530300	6450570	3	Sr1-5	Massive pelitic shist	070/60 N	Large mm to >10 cm Gt in Bi + Chl +/-St
Thackaringa-Pinnacles sz					top to SW	shist
Staurolite ridge						
0520408	6454305	3	TP 1-4	no outcrop. Foliated Cl+Bi	090/steep to S	Large 1cm to <20 cm gt with Chl+Bi +/-St
Thackaringa-Pinnacles sz				shist with V large Gt		
0516204	6454212	3	WTP1	Fairly weathered zone of sheared	090/sub vert	St+Chl+Bi+Sericite (+/- gt) pelitic shist
Thackaringa-Pinnacles sz				psamo-pelitic schist		
0536457	6475491	1	SCS 5-7	Wide zone of highly schistose	070/Sub vert to E	Large St with Qtz+micas+gt
Stephens Crk sz				metapelites and pegmatites	80-90deg stretching lin.	

Appendix 2: Example AX 2000 output file

Calculations for P = 5.0 kbar and T = 500°C

ep Epidopte inc
Symmetric Formalism (TJBH 1998). cz = Al3, ep = Al2Fe, fep = AlFe2 epidote.
Ferric from: Si + Al + Fe(3) = 6 for 12.5 oxygens. Max Ratio = 0.99
SF Model parameters: Wcf = 15.4, Wce = 0.0, Wef = 3.0 kJ. delta H = -26.1 kJ

oxide	wt % cations			activity	±sd	±%
SiO2	37.37	2.996	cz	0.23	0.025	11
TiO2	0	0	ep	0.59	0.059	10
Al2O3	24.32	2.299	fep	0.033	0.0089	27
Cr2O3	0.01	0.001				
Fe2O3	12.4	0.748				
FeO	0.11	0.008				
MnO	1.12	0.076				
MgO	0.01	0.002				
CaO	21.38	1.837				
Na2O	0.13	0.02				
K2O	0.04	0.004				
totals	96.9	7.992				

g Garnet rim
2-site mixing + Regular solution gammas
Ferric from: Cation Sum = 8 for 12 oxygens
W: py.alm=2.5, gr.py=33, py.andr=73, alm.andr=60, spss.andr=60 kJ

oxide	wt % cations			activity	±sd	±%
SiO2	36.72	2.913	py	0.00073	0.000364	50
TiO2	0	0	gr	0.0013	0.00063	48
Al2O3	20.44	1.911	alm	0.15	0.0218	15
Cr2O3	0.03	0.002	spss	0.012	0.00424	36
Fe2O3	4.77	0.285	andr	0.0058308	23525	40
FeO	24.25	1.609				
MnO	10.48	0.704				
MgO	1.75	0.207				
CaO	4.07	0.346				
Na2O	0.12	0.019				
K2O	0.05	0.005				
totals	102.67	8				

chl Chlorite
Ordered Al(M4) model. Holland et al. 1998 EJM
Ferric from: Cation Sum<=10 for 14 oxygens. Max Ratio = 0.2
Wcl-da = 2.5, Wcl-am = 18, Wam-da = 20.5 kJ

oxide	wt % cations			activity	±sd	±%
SiO2	23.98	2.519	clin	0.02	0.0063	31
TiO2	0.1	0.008	daph	0.006	0.00251	42

Al2O3	21.47	2.659	ames	0.045	0.0105	23
Cr2O3	0.03	0.003				
Fe2O3	4.93	0.39				
FeO	21.22	1.864				
MnO	0.35	0.031				
MgO	15.38	2.407				
CaO	0.11	0.013				
Na2O	0.25	0.051				
K2O	0.41	0.055				
totals	88.24	10				

mu Muscovite

HP98 model + nonideal mu-cel-fcel-pa interactions

Ferric from: Tet + Oct cation sum = 6.05 for 11 oxygens. Max Ratio = 0.7

oxide	wt %	cations		activity	±sd	±%
SiO2	47.41	3.101	mu	0.72	0.072	10
TiO2	0.24	0.012	pa	-	-	-
Al2O3	33.6	2.591	cel	0.029	0.0081	27
Cr2O3	0.1	0.005	ma	-	-	-
Fe2O3	0	0				
FeO	3.67	0.201				
MnO	0.1	0.006				
MgO	0.94	0.091				
CaO	0.14	0.01				
Na2O	1.07	0.135				
K2O	12.1	1.011				
totals	99.38	7.162				

bi Biotite

Al-M1 ordered, site-mixing model + macroscopic RS gammas: (ann, phl, east, ob

Ferric from: Tet + Oct cation sum = 6.9 for 11 oxygens. Max Ratio = 0.15

SF model parameters: Wpa=9, Wpe=10, Wpo=3, Wao=6, Wae=-1, Woe=10 (kJ)

oxide	wt %	cations		activity	±sd	±%
SiO2	34.42	2.663	phl	0.062	0.0136	22
TiO2	1.51	0.088	ann	0.113	0.0181	16
Al2O3	16.54	1.509	east	0.053	0.0124	23
Cr2O3	0.02	0.001				
Fe2O3	0	0				
FeO	20.52	1.328				
MnO	0.22	0.015				
MgO	10.43	1.202				
CaO	0.17	0.014				
Na2O	0.43	0.064				
K2O	12.98	1.282				
totals	97.27	8.167				

ilhem Ilmenite matrix

2-site ideal mixing

Ferric from: Cation Sum = 2 for 3 oxygens

oxide	wt %	cations		activity	±sd	±%
SiO2	0.39	0.01	ilm	0.78	0.0779	10
TiO2	48.68	0.937	hem	0.0029	0.00102	36
Al2O3	0.16	0.005	prh	0.089	0.0175	20
Cr2O3	0	0	gei	-	-	-
Fe2O3	5.59	0.108				
FeO	38.87	0.832				
MnO	4.36	0.095				
MgO	0.03	0.001				
CaO	0.27	0.007				
Na2O	0.09	0.005				
K2O	0.04	0.001				
totals	98.48	2				

fsp Plagioclase
Holland & Powell 1992 model 1
Ferric from: all ferric
plag is C1 structure

oxide	wt %	cations		activity	±sd	±%
SiO2	59.53	2.653	an	0.6	0.0302	5
TiO2	0.01	0	ab	0.66	0.0329	5
Al2O3	25.38	1.333				
Cr2O3	0	0				
Fe2O3	0.32	0.011				
FeO	0	0				
MnO	0.08	0.003				
MgO	0	0				
CaO	7.32	0.35				
Na2O	7.47	0.645				
K2O	0.09	0.005				
totals	100.21	5				

Appendix 3: Example thermocalc output file (sample RD-11)

```
THERMOCALC v3.1, (c) Roger Powell and Tim Holland  running at
  14.31 on Wed 1 Oct,2003 with thermodynamic dataset 1999
  produced at Adelaide University


an independent set of reactions has been calculated

Activities and their uncertainties

                 cz       ep      fep       py       gr      alm     spss
a             0.230    0.590   0.0330 0.000730  0.00130    0.150   0.0120
sd(a)/a     0.17787  0.10000  0.40181  0.74522  0.71427  0.19769  0.53508

               andr     daph     ames       mu      cel      phl
a           0.00583  0.00600   0.0450    0.720   0.0290   0.0620
sd(a)/a     0.60518  0.60264  0.37244  0.10000  0.41305  0.33840

                ann     east      ilm      pnt       an        q
a             0.113   0.0530    0.780   0.0890    0.600     1.00
sd(a)/a     0.24013  0.35554  0.09987  0.24898  0.05033        0

                H2O
a              1.00
sd(a)/a

Independent set of reactions
1)  3east + 6q = py + 2mu + phl
2)  phl + 3an = py + gr + mu
3)  2phl + 3an = py + gr + cel + east
4)  2ames + cel + 4phl + 32an = 16cz + 7py + 5mu
5)  36cz + 14py + 10mu = 3ames + 10phl + 72an + 6H2O
6)  24cz + 10alm + 5mu + 3q = 3daph + 5ann + 48an
7)  3daph + 2ann + 24an = 12cz + 7alm + 2mu + 6H2O
8)  24ep + 7gr + 5alm + 3q = 12andr + 3daph + 33an
9)  24fep + 19gr + 5alm + 3q = 24andr + 3daph + 33an
10)  ann + east + 3pnt + 6q = spss + 2cel + 3ilm

Calculations for the independent set of reactions
 at T = 500°C (for x(H2O) = 1.0)
        P(T)   sd(P)       a   sd(a)         b        c     ln_K sd(ln_K)
1        4.5    3.77   45.31   10.06  -0.02276   -3.529   -1.848    1.359
2        4.5    1.00    7.77    0.74   0.11366   -7.144   -9.883    1.101
3        5.6    1.27   17.69    3.53   0.14061   -7.398  -13.252    1.358
4        4.9    0.61 -207.22    5.99   1.01701  -68.306  -38.503    6.381
5        4.9    0.55  798.12   13.32  -2.71335  156.016   83.419   13.292
6        4.9    0.38  785.00   13.28  -1.71634  103.421    5.116    5.738
7        5.5    0.46  -97.80    9.57   0.48552  -51.149    0.396    3.387
8        4.8    0.95  434.93   17.69  -0.77094   67.015  -25.274    9.513
9        4.2    2.11 -289.44   17.56  -0.50915   68.223   61.942   22.252
10       6.0    2.58    8.18    7.22   0.02198   -4.363    0.126    1.342

Average pressures (for x(H2O) = 1.0)

Single end-member diagnostic information

av, sd, fit are result of doubling the uncertainty on ln a :
a ln a suspect if any are v different from lsq values.
e* are ln a residuals normalised to ln a uncertainties :
large absolute values, say >2.5, point to suspect info.
```

hat are the diagonal elements of the hat matrix :
large values, say >0.50, point to influential data.
For 95% confidence, fit (= sd(fit)) < 1.37;
however a larger value may be OK - look at the diagnostics!

	av	sd	fit
lsq	4.33	0.47	1.54

	P	sd	fit	e*	hat	a(obs)	a(calc)
cz	4.23	0.63	1.53	-0.3	0.45	0.230	0.219
ep	4.33	0.48	1.54	-0.0	0.01	0.590	0.588
fep	4.33	0.48	1.54	-0.1	0.04	0.0330	0.0319
py	4.32	0.47	1.52	-0.9	0.00	0.000730	0.000383
gr	4.39	0.47	1.50	1.1	0.05	0.00130	0.00277
alm	4.26	0.46	1.48	-1.0	0.02	0.150	0.123
spss	4.33	0.47	1.54	0.1	0.00	0.0120	0.0125
andr	4.32	0.47	1.54	0.2	0.01	0.00583	0.00670
daph	4.36	0.35	1.15	3.0	0.00	0.0200	0.0745
ames	4.32	0.48	1.54	-0.1	0.01	0.00600	0.00552
mu	4.38	0.48	1.52	0.5	0.02	0.0450	0.0534
cel	4.30	0.44	1.43	-1.8	0.00	0.720	0.601
phl	4.26	0.46	1.48	1.1	0.02	0.0290	0.0452
ann	4.41	0.48	1.50	-0.8	0.04	0.0620	0.0473
east	4.33	0.47	1.54	-0.0	0.00	0.113	0.112
ilm	4.33	0.47	1.54	0.0	0.00	0.0530	0.0538
pnt	4.33	0.47	1.54	-0.1	0.00	0.780	0.772
an	4.36	0.61	1.54	-0.1	0.23	0.00290	0.00280
q	4.33	0.47	1.54	0	0	0.0890	0.0890
H2O	4.33	0.47	1.54	0	0	0.600	0.600

T°C	400	425	450	475	500	525	550	575	600
av P	-	-	3.0	3.7	4.3	5.0	5.7	6.3	+
sd	1.06	0.89	0.73	0.59	0.47	0.41	0.43	0.52	0.65
sigfit	3.9	3.2	2.5	2.0	1.5	1.3	1.3	1.6	1.9

****

an independent set of reactions has been calculated

Activities and their uncertainties

	py	gr	alm	spss	andr	cz	ep
a	0.000650	0.00140	0.140	0.0130	0.00549	0.240	0.580
sd(a)/a	0.75083	0.70990	0.20801	0.52652	0.61053	0.17328	0.10000

	fep	daph	ames	phl	ann	east
a	0.0310	0.00920	0.0390	0.0680	0.0700	0.0610
sd(a)/a	0.40732	0.56235	0.38642	0.32788	0.31103	0.34022

	ilm	pnt	mu	cel	q
a	0.720	0.0740	0.650	0.0260	1.00
sd(a)/a	0.09944	0.25724	0.10000	0.42211	0

	H2O
a	1.00
sd(a)/a	

Independent set of reactions

1) 8gr + 15ames + 42q = 20py + 12cz + 54H2O
2) 12cz + 15daph + 18q = 8gr + 25alm + 66H2O
3) 2ames + phl + 4q = 3py + east + 8H2O
4) 3ames + phl + 9q = 5py + mu + 12H2O
5) 2east + 6q = py + mu + cel
6) 3daph + mu + 3q = 4alm + ann + 12H2O
7) gr + fep = andr + cz
8) gr + 2fep = andr + 2ep
9) py + ann + 3pnt = spss + phl + 3ilm

Calculations for the independent set of reactions
at P = 5.0 kbar(for x(H2O) = 1.0)

	T(P)	sd(T)	a	sd(a)	b	c	ln_K	sd(ln_K)
1	529.4	31	3294.75	10.43	-3.56565	-3.168	-62.663	17.195
2	545.9	22	3263.42	40.05	-3.85596	-1.552	-14.269	11.609
3	523.1	32	502.46	3.58	-0.50110	-0.011	-15.636	2.428
4	519.5	33	776.35	1.93	-0.76304	-1.781	-24.703	3.944
5	547.3	2341	55.22	6.76	0.00418	-3.783	-5.825	1.102
6	562.4	20	589.41	7.80	-0.74529	1.124	3.973	1.909
7	417.9	310	-35.11	0.73	0.02162	0.081	3.412	1.036
8	457.6	375	-60.36	1.32	0.02182	0.101	7.224	1.257
9	537.5	1146	-56.96	6.20	-0.00915	-0.325	9.792	1.315

Average temperatures (for x(H2O) = 1.0)

Single end-member diagnostic information

av, sd, fit are result of doubling the uncertainty on ln a :
a ln a suspect if any are v different from lsq values.
e* are ln a residuals normalised to ln a uncertainties :
large absolute values, say >2.5, point to suspect info.
hat are the diagonal elements of the hat matrix :
large values, say >0.47, point to influential data.
For 95% confidence, fit (= sd(fit)) < 1.39;
however a larger value may be OK - look at the diagnostics!

	av	sd	fit
lsq	534	15	1.03

	T	sd	fit	e*	hat	a(obs)	a(calc)
py	537	16	1.02	0.5	0.21	0.000650	0.000951
gr	535	14	0.96	1.2	0.00	0.00140	0.00320
alm	531	17	1.03	-0.2	0.15	0.140	0.133
spss	534	15	1.03	-0.0	0.00	0.0130	0.0129
andr	534	15	1.03	0.2	0.00	0.00549	0.00638
cz	534	14	1.02	-0.3	0.00	0.240	0.228
ep	534	15	1.03	-0.2	0.00	0.580	0.568
fep	535	15	1.03	0.2	0.02	0.0310	0.0343
daph	523	15	0.92	1.1	0.24	0.0180	0.0291
ames	539	16	1.01	-0.5	0.12	0.00920	0.00711
phl	537	14	0.97	0.8	0.03	0.0390	0.0539
ann	536	14	1.00	-0.6	0.02	0.0680	0.0557
east	534	15	1.03	-0.1	0.01	0.0700	0.0673
ilm	534	15	1.03	-0.0	0.00	0.0610	0.0608
pnt	534	15	1.03	0.0	0.00	0.720	0.722
mu	534	14	1.01	0.4	0.00	0.00380	0.00468
cel	536	12	0.85	-1.8	0.01	0.0740	0.0470
q	534	15	1.03	0	0	0.00210	0.00210
H2O	534	15	1.03	0	0	0.650	0.650

P	4.0	4.2	4.5	4.8	5.0	5.2	5.5	5.8	6.0
av T	532.0	532.8	533.3	533.8	534.1	534.3	534.4	534.4	534.4
sd	15	15	15	15	15	15	14	15	15
sigfit	1.1	1.1	1.1	1.0	1.0	1.0	1.0	1.0	1.0

****

Appendix 4: Garnet Sm-Nd data

Mutooroo RSZ

	Sm (ppm)	Nd (ppm)	$^{147}Sm/^{144}Nd$	$^{143}Nd/^{144}Nd$	± (2SE)	
WR	2.580	12.431	0.125	0.51161257	0.000014	Age = 517 ± 14 Ma
gt1	0.977	1.779	0.332	0.51231094	0.000013	Initial 143Nd/144Nd =0.511186 ± 0.000023
gt2	1.951	5.266	0.224	0.51193668	0.000018	MSWD = 0.81

Thackaringa -Pinnacles RSZ

	Sm (ppm)	Nd (ppm)	$^{147}Sm/^{144}Nd$	$^{143}Nd/^{144}Nd$	±	
gt core1	2.337	3.043	0.464	0.51274409	0.000009	Age = 499.8 ± 9.8 Ma
gt rim 1	1.735	0.833	1.258	0.51534330	0.000049	Initial 143Nd/144Nd =0.511224 ± 0.000033

Kings Dam RSZ

	Sm (ppm)	Nd (ppm)	$^{147}Sm/^{144}Nd$	$^{143}Nd/^{144}Nd$	±	
WR	1.187	6.444	0.111	0.51143341	0.000009	Age = 505 ± 13 Ma
gt1	0.395	0.376	0.636	0.51314706	0.000054	Initial 143Nd/144Nd =0.511067 ± 0.000014
gt2	0.650	3.066	0.128	0.51148454	0.000028	MSWD = 1.3
gt2 leachate	0.296	0.656	0.273	0.51194582	0.000061	
gt3	0.825	3.113	0.160	0.51160885	0.000016	
gt3 leachate	0.122	0.130	0.566	0.51299142	0.000085	